aptara | MIM | mim'017 | Dispatch: February 5, 2008 | CE: IV
Journal | MSP No. | No. of pages: 13 | PE: Caroline

Microbiol Immunol 2008; **52**: 1–13
doi:10.1111/j.2008.1432-1033.00017.x

ORIGINAL ARTICLE

Disruption of the association of 73 kDa heat shock cognate protein with transporters associated with antigen processing (TAP) decreases TAP-dependent translocation of antigenic peptides into the endoplasmic reticulum

Kenjiro Kamiguchi[1], Toshihiko Torigoe[2], Osamutaro Fujiwara[2], Shin Ohshima[2], Yoshihiko Hirohashi[2], Hiroeki Sahara[2], Itaru Hirai[2], Yutaka Kohgo[1] and Noriyuki Sato[2]

[1]Third Department of Internal Medicine, Asahikawa Medical College, Asahikawa, and [2]Department of Pathology (Section 1), Sapporo Medical University School of Medicine, Sapporo, Japan

Correspondence
Toshihiko Torigoe, Department of Pathology, Sapporo Medical University School of Medicine, S-1, W-17, Chuo-ku, Sapporo 060-8556, Japan.
Tel: +81 11 611 2111 (ext. 2691);
fax: +81 11 643 2310;
email: torigoe@sapmed.ac.jp

Received: 23 October 2007; accepted: 16 November 2007

List of Abbreviations: ATPase, ATP phosphatase; CHAPS, 3-[(cholamidopropyl) dimethylammonio]-1-propanesulfonic acid; 15-DSG, 15-deoxyspergualin; ER, endoplasmic reticulum; HSC73, 73 kDa heat shock cognate protein; HSP70, 70 kDa heat shock protein; HSP90, 90 kDa heat shock protein; MeDSG, methyldeoxyspergualin; MHC, major histocompatibility complex; RCMLA, reduced carboxymethylated lactalbumin; TAP, transporters associated with antigen processing.

Key words
antigen presentation, deoxyspergualin, heat shock protein, major histocompatibility complex.

ABSTRACT

Major histocompatibility complex class I-bound antigenic peptides generated in the cytosol are translocated into the ER by TAP. In the present study, the physical association of HSC73 with TAP in human lymphoblastoid T1 cells was demonstrated. The dissociation was induced in the presence of 10 mM ATP, indicating that the ADP-binding form of HSC73 might be associated with TAP. We found that HSC73-binding immunosuppressant, MeDSG disrupted the HSC73-TAP association, whereas it did not affect the binding of HSC73 to a substrate protein. MHC class I expression on the cell surface was also downregulated. Then, the effect of MeDSG on the TAP-mediated ER translocation was examined using two homologous model peptides, NGT-Bw4 and NGT-Bw6, which had distinct binding affinity to HSC73. Although high-affinity peptide NGT-Bw4 was translocated by TAP, low-affinity peptide NGT-Bw6 was not. The TAP-dependent translocation of NGT-Bw4 was abolished in the presence of MeDSG. Decreased presentation on the cell surface was shown for the human leukocyte antigen (HLA)-A31-restricted natural antigenic peptide F4.2, which had high affinity to HSC73, in the presence of MeDSG. It was indicated that disruption of the HSC73-TAP association resulted in inhibition of TAP-dependent translocation of HSC73-bound peptides. Our findings highlighted an important role of HSC73 for feeding antigenic peptides to TAP, and suggested a possibility that a synthetic polyamine might inhibit the function of HSC73, thereby suppressing MHC class I-restricted presentation of HSC73-bound antigenic peptides.

Major histocompatibility complex class I molecules bind to endogenous antigenic peptides and present them to CD8-positive T cells. Most of the peptides are produced by proteasome-mediated degradation of cytosolic or nuclear proteins (1). The degradation products are transported from the cytosol into the endoplasmic reticulum (ER) by heterodimeric transmembrane molecules called TAP, and then loaded onto MHC class I molecules (2–4). The mechanism of peptide transfer from TAP to MHC class I has been well documented. TAP1 and TAP2 belong to a family of ATP-binding cassette transporters, and can translocate peptide fragments into the ER through hydrolysis of ATP (5, 6). The transfer of translocated peptides to MHC class I requires a complex formation among TAP, empty MHC

heavy chain and tapasin (7–11). Although tapasin does not bind to peptides, it is an essential molecule for the physical association between TAP and MHC heavy chain (12). It is known that some molecular chaperones such as calnexin (9), calreticulin (13, 10), ERp57 (14, 15) and GRP94 (16) have important roles during assembly and maturation of MHC class I complex. In contrast to the ER event, the mechanism of peptide transfer in the cytosol remains to be elucidated. How can peptide fragments produced by proteasome be transported to the TAP? What molecules are associated with the cytosolic domain of TAP? It has been speculated so far that the cytosolic peptide fragments should be accompanied by some molecular chaperones before TAP-dependent translocation so that: (i) hydrophobic peptides become soluble in the cytosol; and (ii) peptides can be protected from degradation by cytosolic peptidases (17). Moreover, it is possible that antigenic peptides may be transported through an energy-dependent active mechanism rather than through a passive diffusible mechanism.

Previously our group and others have shown that heat shock proteins (HSP) were associated with antigenic peptides, and that some of them were presented to T cells (18–22). It was indicated that HSP-chaperoned peptides might be efficiently presented by MHC class I (23). One of the 70 kDa HSP family proteins, HSC73, is a cytoplasmic protein serving as a molecular chaperone. HSC73 can bind to various peptides or proteins (24, 25), preferentially containing hydrophobic amino acids, and functions to regulate localization, conformation, and degradation of these molecules (26). HSC73 has an ATP-binding domain, and its function is dependent on the intrinsic ATPase activity (27). These data led us to speculate that HSC73 might be involved in the feeding of cytosolic peptides to TAP.

In the present study, we focused on the functional significance of the interaction between TAP1 and HSC73 for TAP-dependent peptide translocation. We found that HSC73 was associated with TAP1 in an ATP-dependent manner and that the association was disrupted by HSC73-binding polyamine compound, MeDSG (28, 29). 15-DSG is an immunosuppressant that has been used clinically to protect against rejection after organ transplantation (30, 31). MeDSG induced the downregulation of cell surface MHC class I levels. The consequences of the dissociation of HSC73 from TAP were analyzed by ER translocation assay of synthetic peptides and by cytotoxic T lymphocyte (CTL) assay against endogenous human leukocyte antigen (HLA)-A31-restricted natural antigenic peptides (32). We demonstrated that TAP-mediated translocation and presentation of HSC73-bound peptides were abolished in the presence of MeDSG. Our study provided evidence for the direct involvement of a molecular chaperone, HSC73, in the feeding of antigenic peptides into TAP and the inhibitory role of polyamine compound.

MATERIALS AND METHODS

Cells, antibodies, peptides and reagents

Human lymphoblastoid cell line T1 cells and TAP-deficient cell line T2 cells (33) were purchased from American Type Culture Collection (Manassas, VA, USA). These cells were cultured in RPMI-1640 medium (Gibco BRL, Gaithersburg, MD, USA) supplemented with 100 U/mL penicillin, 100 mg/mL streptomycin, 2 mM L-glutamine and 10% FCS (Filtron, Brooklyn, Victoria, Australia). In some cases, T1 cells were cultured in the complete media containing 150 U/mL γ-interferon (IFN-γ; Chugai Pharmaceutical, Tokyo, Japan).

A gastric signet ring cell carcinoma line, HST-2, and $CD8^+$ CTL clone, TcHST-2, were established and characterized previously (34). TcHST-2 is specifically cytotoxic to autologous HST-2 cells in the context of HLA-A31 restriction, as this cytotoxicity was completely blocked by anti-HLA-A31 mAb, as previously reported. TcHST-2 was maintained in an AIM-V serum-free medium (Gibco BRL) supplemented with 100 U/mL recombinant interleukin (IL)-2. We also used HLA-$A31^+$ lines, such as C1R-A31 (B lymphoma line C1R transfected with genomic HLA-A*31012 DNA) and HOBC8-A31-12 (HOBC8 cells transfected with HLA-A*31012 cDNA). Establishment and characterization of these cells were reported previously (32).

Affinity purified rabbit anti-human TAP1 polyclonal antibody R.RING4C was kindly provided by Dr P. Cresswell (Yale University, New Haven, CT, USA). Anti-HSP70 mAb 3a3 was purchased from Affinity BioReagents (Neshanic Station, NJ, USA).

Amino acid sequences of NGT-Bw4 peptide (sequence, NGTRENLRIALRY) and NGT-Bw6 peptide (sequence, NGTRESLRNLRGY) are derived from the common epitope of α1-domain of human MHC class I heavy chain (35) with additional N-terminal *N*-glycosylation motif. F4.2 peptide (sequence, YSWMDISCWI) was identified as HLA-A31-restricted tumor antigen peptide recognized by TcHST-2 cells, as previously reported (32). These peptides were synthesized, purified by high performance liquid chromatography (HPLC) and confirmed by mass spectrometry (Iwaki Glass Life Science Center, Chiba, Japan).

MeDSG (28) was provided by Nippon Kayaku Co. (Tokyo, Japan). Spermidine was purchased from Wako Chemical Co. (Osaka, Japan). RCMLA was purchased from Sigma-Aldrich Co. (St Louis, MO, USA). Bovine

brain 70 kDa heat shock protein consisting mainly of HSC73 was purchased from StressGen (Victoria, BC, Canada).

Immunoprecipitation

5×10^6 cells were washed once with ice-cold phosphate-buffered saline (PBS) and lysed in 500 μL of 0.5% CHAPS lysis buffer (0.5% 3-[(cholamidopropyl) dimethylammonio]-1-propanesulfonic acid (CHAPS), 50 mM Tris-HCl, pH 7.5, 150 mM NaCl, 5 mM $MgCl_2$, 1 mM phenylmethylsulfonyl fluoride, 0.2 TIU/mL aprotinin). After incubation on ice for 45 min, nuclei and cell debris were removed by centrifugation (15 000 × g, 10 min). The lysates were pre-cleared by incubating for 1 hr with rabbit immunoglobulin G (IgG) conjugated with fixed *Staphylococcus aureus* (Sigma-Aldrich Co.). Then, the lysates were incubated with 2.7 μg anti-TAP1 antibody at 4 °C for 30 min, followed by incubation with 25 μL Protein A-Sepharose beads (Pharmacia Biotech, Uppsala, Sweden) for 18 hr. After washing four times with lysis buffer, immunoprecipitates were boiled for 5 min with reducing sodium dodecylsulfate (SDS) sample buffer (3% SDS, 0.5 M 2-mercaptoethanol, 10% glycerol, 62.5 mM Tris-HCl (pH 6.8)), and subjected to 8% SDS-polyacrylamide gel electrophoresis (PAGE). In some cases, MeDSG or spermidine was included in the cell lysates at a final concentration of 200 μg/mL before incubating with the antibody.

Western blotting

Proteins separated by SDS-PAGE were transferred onto Immobilon membranes (Millipore, Bedford, MA, USA). The membranes were soaked in a blocking buffer (PBS, 10% non-fat dry milk) for 2 hr at room temperature. Then, the blots were incubated for 90 min with anti-TAP1 antibody or anti-HSP70 antibody 3a3. After washing in a washing buffer (PBS, 0.1% Tween-20), the membranes were incubated with horseradish peroxidase-labeled anti-rabbit (KPL, Gaithersburg, MD, USA) or anti-mouse antibodies (KPL) for 30 min, followed by incubation in ECL detection fluid (Amersham, Birmingham, AL, USA) for 1 min. The bands were visualized using X-ray films (Fuji Photo Film, Tokyo, Japan). In some cases, membranes were incubated in a stripping buffer (62.5 mM Tris-HCl, pH 7.5, 2% SDS, 0.1 M 2-mercaptoethanol) for 30 min at 50 °C, rinsed in a washing buffer and soaked in a blocking buffer again for 1 hr before incubating with antibody.

Flow cytometry

Cells were cultured for 36 hr in an AIM-V serum-free medium containing various concentrations of MeDSG. After washing once with PBS, cells were incubated with anti-human MHC class I antibody W6/32 for 45 min at 4 °C, followed by incubation with fluorescein-isothiocyanate (FITC)-labeled anti-mouse IgG antibody (KPL) for 45 min and analysis on a FACScan flow cytometer (Becton Dickinson, Mountain View, CA, USA).

Complex formation between HSC73 and RCMLA, and competitive HSC73-binding assay of synthetic peptides

The binding affinity of HSC73 to a substrate protein was assessed as described by Fourie *et al.*, based on observations that HSC73 binds to an unfolded form of lactalbumin (RCMLA) (36). RCMLA (250 μg) was incubated with 37 mBq of 125-iodine (MEN Life Science Products, Boston, MA, USA) and two drops of Iodo-beads (Pierce, Rockford, IL, USA) in 250 μL PBS for 15 min at 20 °C. Then, labeled RCMLA was separated from free 125-iodine by a Micro Spin G-25 column (Pharmacia Biotech). The final concentration of the labeled RCMLA was analyzed by micro BCA assay (Pierce). The specific radioactivity was 4.8×10^6 c.p.m./μg. HSC73 (2 μg; 2.8 μM final concentration) was incubated with 40 ng labeled RCMLA in 10 μL PBS (HSC73/RCMLA mole ratio of 10:1) at 37 °C for 1 hr in the absence or presence of various concentrations of MeDSG or spermidine. In the case of competitive binding assay of peptides, 2.8 μM, 28 μM, 84 μM or 140 μM of each peptide was incubated with the HSC73-RCMLA mixture. Free RCMLA was separated from HSC73-bound RCMLA by native PAGE (resolving gel: 7% acrylamide, 0.4 M Tris-HCl, pH 8.8; running buffer: 25 mM Tris-HCl, 192 mM glycine, pH 8.3), followed by autoradiography using X-ray films.

Radiolabeling and ER translocation assays of synthetic peptides

Synthetic peptides (750 μg) were resolved in 250 μL PBS containing 20% acetonitril. The peptides were labeled with 125-iodine and purified as described above. The specific radioactivities of the peptides were 1×10^6 c.p.m./μg for both NGT-Bw4 and NGT-Bw6 peptides.

ER translocation assay was carried out as described by Androlewicz *et al.* (37). Briefly, 1×10^7 cells were washed with serum-free RPMI-1690 medium and permeabilized by incubation in the medium containing 4 mM dithiothreitol and 1 U/mL streptolysin O (Murex, Norcross, GA, USA) at 4 °C for 10 min. After washing cells with serum-free medium three times, the permeabilized cells were incubated with 19 μM radiolabeled peptide and 4 mg/mL BSA in 1 mL transport buffer (50 mM Hepes, pH 7.0, 78 mM KCl, 4 mM $MgCl_2$, 8.37 mM $CaCl_2$, 10 mM ethylene glycol-bis[beta-aminoethyl ether]-*N*,*N*,*N*′,*N*′-tetraacetic acid [EGTA], 1 mM dithiothreitol) containing

1 mM ATP at 37 °C. The reaction was terminated by washing cells with ice-cold transport buffer, followed by lysis in a lysis buffer (10 mM Tris-HCl, pH 7.4, 1% Triton X-100, 150 mM NaCl, 5 mM iodoacetamide, 0.5 mM phenylmethylsulfonyl fluoride). Then, cell lysates were purified by centrifugation at 10 000 × g for 5 min. Glycosylated peptides were collected by incubating 100 μL Con-A Sepharose beads (Pharmacia Biotech) with the lysates at 4 °C for 60 min. After washing the beads with lysis buffer five times, radioactivities of the beads were analyzed by a gamma counter.

Minigene construction, transfection and cytotoxicity assays

In order to express peptide antigen F4.2 in endogenous form, we constructed expression minigene vectors, pF4.2, pF4.2ss and pF4.2reverse. pcDSRα-E3 contains an adenovirus E3/19 kDa protein signal sequence (38) under the control of the SRα promoter. pF4.2ss was constructed by insertion of oligonucleotides corresponding to F4.2 peptide into the *Pst*I and *Xba*I sites of the pcDSRα-E3 expression vector. pF4.2 and pF4.2reverse were constructed by insertion of the F4.2-coding oligonucleotides into the *Eco*RI site of the pcDSRα expression vector in a sense orientation or an antisense orientation, respectively. Expression vectors were transfected to HOBC8-A31-12 cells or C1R-A31 cells by using Lipofectin reagent (Life Technologies, Gaithersburg, MD, USA) and cultured in the AIM-V serum-free media. In some cases, 200 μg/mL MeDSG was included in the media. Forty-eight hours after the transfection, cells were mixed with TcHST-2 cells for 10 hr at an E/T ratio of 3:1 or 10:1, followed by quantification of tumor necrosis factor (TNF) production. In the case of the ^{51}Cr release assay, target cells were labeled with ^{51}Cr for 1 hr, washed with PBS and co-cultured with TcHST-2 for 10 hr at an E/T ratio of 10:1 in the presence or absence of 200 μg/mL MeDSG, followed by counting radioactivities of ^{51}Cr in the culture supernatants. The expression of the oligonucleotide sequence coding F4.2 in the transfected cells was confirmed by using polymerase chain reaction (PCR) analysis.

RESULTS

HSC73 is co-immunoprecipitated with TAP1

It is known that MHC class I is associated with TAP1 in the ER until antigenic peptides are loaded on the MHC class I molecule (8). Analogously, we speculated that HSP70 might be associated with TAP1 in the cytoplasm. TAP1 (70 kDa) was immunoprecipitated from the lysate of human lymphoblastoid cell line T1 cells but not from the lysate of TAP-deficient line T2 cells, as detected by immunoblotting using anti-TAP1 antibody (Fig. 1a). The same immunoprecipitates were examined to detect HSC73. Although similar levels of HSC73 expression were demonstrated by immunoblotting of T1 lysates and T2 lysates with anti-HSP70 antibody (Fig. 1b, lanes 1,2), HSC73 was detected only in the TAP1-immunoprecipitates from T1 cell lysates (Fig. 1b,

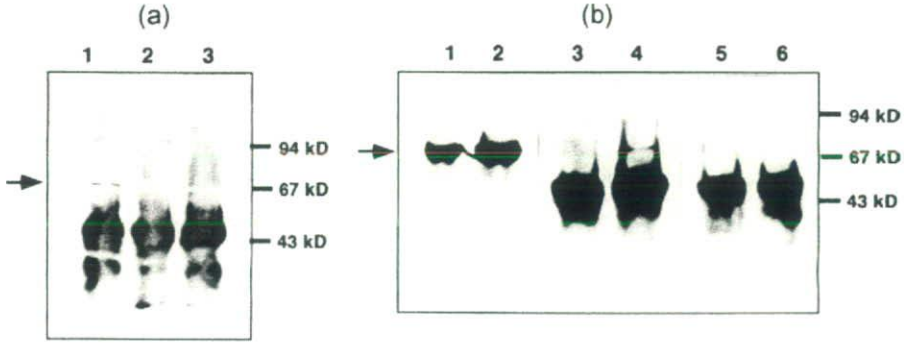

Fig. 1. Co-immunoprecipitation of HSC73 with TAP1 from T1 cell lysates. (a) T1 cells (lanes 1, 2) or T2 cells (lane 3) were lysed by 0.5% CHAPS lysis buffer. The lysates were immunoprecipitated with anti-TAP1 antibody (lanes 1, 3) or control antibody (lane 2). The immunoprecipitates were resolved by 8% sodium dodecylsulfate-polyacrylamide gel electrophoresis (SDS-PAGE), transferred to polyvinylidine difluoride (PVDF) membranes and analyzed by immunoblotting with anti-TAP1 antibody. Arrowhead indicates the 70 kDa TAP1. (b) T2 lysates (lane 1) or T1 lysates (lane 2) were resolved by 8% SDS-PAGE and analyzed by immunoblotting with anti-HSP70 antibody. In lanes 3–6, immunoprecipitates with anti-TAP1 antibody (lanes 3, 4) or control antibody (lanes 5, 6) were made from T2 lysates (lanes 3, 5) or T1 lysates (lanes 4, 6), resolved by 8% SDS-PAGE and analyzed by immunoblotting with anti-HSP70 antibody. The faster-migrating 50 kDa band in each lane is an immunoglobulin heavy chain. The band corresponding to 73 kDa HSC73 is indicated by an arrowhead.

lanes 3,4). As no band of HSC73 was detected in the immunoprecipitates with normal rabbit IgG (Fig. 1b, lanes 5,6), it is indicated that HSC73 is associated with TAP1 in T1 cells.

ATP-dependent dissociation of HSC73 from TAP1

HSC73 has an ATP-binding domain and an intrinsic ATPase activity. It can form at least two conformations, the ATP-binding form and the ADP-binding form. It is known that HSC73 can bind to and dissociate from other molecules depending upon the ATP/ADP-dependent conformational change (39). To test if the association of HSC73 with TAP1 is regulated by ATP, TAP1 was immunoprecipitated from T1 cell lysates in the presence of various concentrations of ATP or apyrase, which hydrolyzed ATP. The addition of ATP can facilitate the formation of the ATP-binding conformation of HSC73, whereas hydrolysis of ATP can facilitate the ADP-binding conformation. T1 cells were cultured in the medium supplemented with 150 U/mL IFN-γ for 48 hr before lysis in order to increase the level of TAP1 expression.

As shown in Figure 2a, similar levels of TAP1 were immunoprecipitated from T1 cell lysates in the presence of ATP or apyrase. Remarkably, the co-precipitation of HSC73 with TAP1 was decreased when 1 mM or 10 mM ATP was added to the cell lysates (Fig. 2b, lanes 2,3). In contrast, depletion of ATP from cell lysates by apyrase did not affect the co-immunoprecipitation levels of HSC73 (Fig. 2b, lanes 4,5). These data imply that the ADP-binding form of HSC73 may have higher affinity to TAP1 than its ATP-binding form.

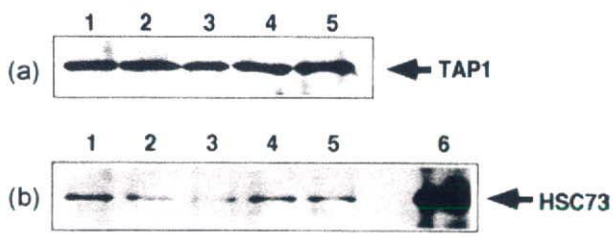

Fig. 2. ATP-dependent dissociation of HSC73 from TAP1. T1 cells were cultured in complete media containing 150 U/mL γ-interferon for 24 hr and lysed by 0.5% CHAPS lysis buffer. TAP1 was immunoprecipitated from the lysates using anti-TAP1 antibody under the condition of the absence (lane 1) or presence of 1 mM ATP (lane 2), 10 mM ATP (lane 3), 1 U/mL apyrase (lane 4) or 10 U/mL apyrase (lane 5). (a) TAP1-immunoprecipitates were resolved by 8% sodium dodecylsulfate-polyacrylamide gel electrophoresis (SDS-PAGE) and analyzed by immunoblotting with anti-TAP1 antibody. (b) TAP1-immunoprecipitates or T1 lysates (lane 6) were resolved by SDS-PAGE and analyzed by immunoblotting with anti-HSP70 antibody.

MeDSG downregulates the cell surface MHC class I levels in T1 cells

In order to know the functional significance of the HSC73/TAP1 interaction, we used a stable derivative of a polyamine compound 15-DSG, which contains a spermidine-like structure. 15-DSG acts as an immunosuppressant and has already been used clinically to suppress rejection after organ transplantation (30). There have been a number of reports demonstrating that 15-DSG could inhibit the MHC class I and/or class II expression in some tissues (40–42). Although the molecular mechanism of the immunosuppressive action of 15-DSG remains obscure, it has been revealed that 15-DSG could specifically bind to both HSC73 and HSP90 (29, 43). Thus, we speculated that 15-DSG might affect the function of HSC73 in the presentation of antigenic peptides. In our experiments MeDSG, a methoxy-derivative of 15-DSG, was used, as it is more stable *in vitro* than 15-DSG (44).

T1 cells were cultured for 36 hr in a serum-free medium containing various concentrations of MeDSG, followed by fluorescent activated cell sorting (FACS) analysis of the cell surface levels of MHC class I expression. As shown in Figure 3a, the cell surface levels of MHC class I were downregulated by the treatment with MeDSG. The downregulation was shown to be dependent on the concentration of MeDSG. In another experiment, the levels of MHC class I were compared between T1 cells and TAP-deficient counterpart T2 cells (Fig. 3b). It is noteworthy that the decreased level of MHC class I expression after the treatment

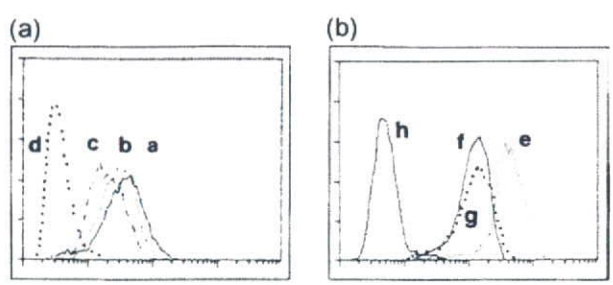

Fig. 3. MeDSG was capable of downregulating the expression of MHC class I molecules on the cell surface of T1 cells. Cells were cultured for 36 hr in AIM-V serum-free media containing various concentrations of MeDSG. After washing once with phosphate-buffered saline (PBS), cells were incubated with anti-human MHC class I antibody W6/32 for 45 min at 4 °C, followed by an incubation with fluorescein-isothiocyanate (FITC)-labeled anti-mouse IgG antibody and an analysis on a FACScan flow cytometer. (a) T1 cells cultivated in the media containing various concentrations of MeDSG (a. 0 μg/mL, b. 100 μg/mL, c. 200 μg/mL) were analyzed for the cell surface expression of MHC class I molecules (d. FITC-labeled anti-mouse IgG antibody only). (b) T1 cells cultivated in the absence (e.) or presence of 200 μg/mL MeDSG (g.) or T2 cells (f.) were analyzed for the cell surface expression of MHC class I molecules (h. FITC-labeled anti-mouse IgG antibody only).

Q3

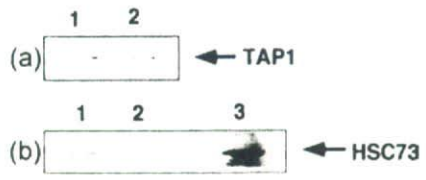

Fig. 4. HSC73 is dissociated from TAP1 in the presence of MeDSG. T1 cells were cultured in media supplemented with 200 μg/mL spermidine or 200 μg/mL MeDSG for 36 hr and lysed by 0.5% CHAPS lysis buffer. TAP1 was immunoprecipitated from the lysates using anti-TAP1 antibody in the presence of 200 μg/mL spermidine (lane 1) or 200 μg/mL MeDSG (lane 2). (a) TAP1-immunoprecipitates from T1 lysates containing spermidine (lane 1) or MeDSG (lane 2) were resolved by sodium dodecylsulfate-polyacrylamide gel electrophoresis (SDS-PAGE) and analyzed for the relative levels of TAP1 by immunoblotting using anti-TAP1 antibody. The band corresponding to TAP1 is indicated. (b) The immunoblot used in (a) was regenerated by soaking in a stripping buffer and reblocking. T1 lysates (lane 3) and TAP1-immunoprecipitates from T1 lysates containing spermidine (lane 1) or MeDSG (lane 2) were analyzed by immunoblotting with anti-HSP70 antibody. The band corresponding to HSC73 is indicated.

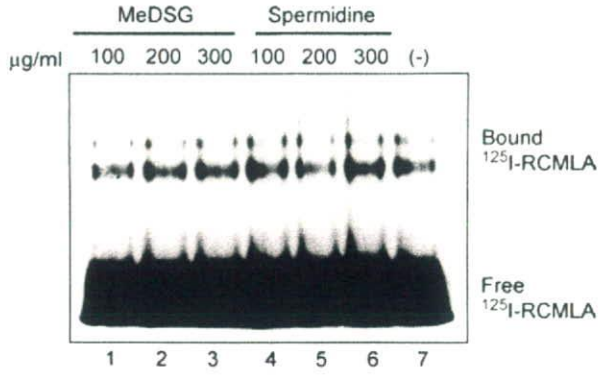

Fig. 5. MeDSG does not affect the interaction between HSC73 and a substrate protein. RCMLA was labeled with 125-iodine by Iodo-beads in 250 μL phosphate-buffered saline (PBS) for 15 min at 20 °C. Radiolabeled RCMLA (40 ng) was incubated with 2 μg HSC73 (HSC73/RCMLA mole ratio of 10:1) in 10 μL PBS at 37 °C for 1 hr in the absence (lane 7) or presence of the indicated concentrations of MeDSG (lanes 1–3) or spermidine (lanes 4–6) and resolved by 7% native polyacrylamide gel electrophoresis (PAGE). Radiolabeled RCMLA was visualized by autoradiography of 125-iodine. The slower-migrating bands correspond to HSC73-bound RCMLA.

with 200 μg/mL MeDSG was comparable to the level in T2 cells (approximately 35% lower level). These data indicate that MeDSG might change T1 cells to T2-like phenotypes possibly by impairing TAP-dependent transportation of MHC class I antigenic peptides.

MeDSG disrupts the association of HSC73 with TAP1

As one of the major intracellular target molecules of MeDSG is HSC73 (29), we examined the effect of MeDSG on the interaction between HSC73 and TAP1. Spermidine, an analogous polyamine compound, was used as a negative control reagent, as it has a low affinity to HSC73 and has less immunosuppressive activity (43).

TAP1 was immunoprecipitated from T1 cell lysates in the presence of 200 μg/mL spermidine or 200 μg/mL MeDSG. These concentrations had been shown to down-regulate the MHC class I expression of T1 cells (Fig. 3a). The levels of TAP1 immunoprecipitated were identical between the spermidine treatment and the MeDSG treatment as detected by western blotting (Fig. 4a). The same blot was then regenerated and was examined to detect HSC73 by western blotting. Strikingly, HSC73 was not detected in the TAP1-immunoprecipitates from T1 cell lysates treated with MeDSG, whereas it was co-precipitated with TAP1 from the lysates treated with spermidine (Fig. 4b). As protein levels of HSC73 contained in the cell lysates were equal between these cases (data not shown), the data imply that MeDSG can disrupt the association of HSC73 with TAP1, possibly by direct binding to HSC73.

MeDSG does not affect the interaction between HSC73 and a substrate protein

It is well known that HSC73 binds to an unfolded form of lactalbumin, RCMLA, through the C-terminal substrate binding domain. In order to know whether MeDSG can affect the interaction between HSC73 and a substrate protein, we analyzed a direct association between HSC73 and radiolabeled RCMLA in the absence or presence of MeDSG. In native PAGE analysis, HSC73-bound RCMLA was detected as the slower migration band (Fig. 5, lane 7). In the presence of MeDSG at concentrations from 100 μg/mL to 300 μg/mL, the levels of HSC73-bound RCMLA were not changed (Fig. 5, lanes 1–3). A control polyamine, spermidine, also failed to affect the binding affinity (Fig. 5, lanes 4–6). These data indicate that MeDSG does not bind to a substrate-binding region on HSC73 and the interaction between HSC73 and TAP1 may be mediated by a different region from the substrate-binding region.

HSC73-binding assay of synthetic peptides

We have reported that peptides Bw4 and Bw6 have distinct binding affinity to HSC73, although they have very homologous amino acid sequences (35, 45). We designed the model peptides NGT-Bw4 and NGT-Bw6 by the addition of an *N*-linked glycosylation site, NGT, to Bw4 and Bw6, respectively so that the ER-translocated peptides could be collected by Con A Sepharose beads. HSC73-binding affinity of the model peptide was assessed by

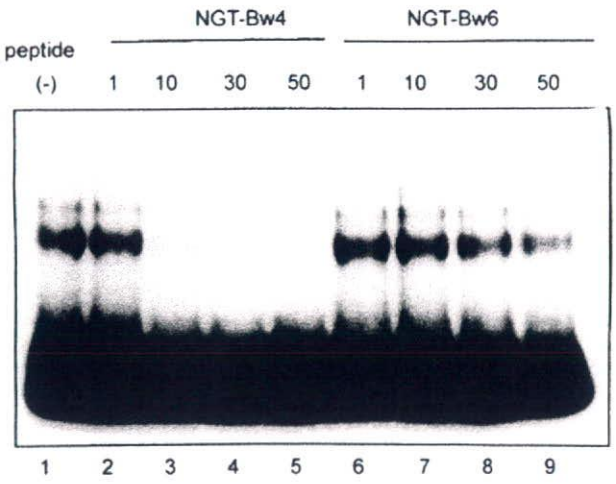

Fig. 6. HSC73-binding assay of synthetic peptides. RCMLA was labeled with 125-iodine by Iodo-beads as described earlier. Radiolabeled RCMLA (40 ng) was incubated with 2 μg HSC73 (HSC73/RCMLA mole ratio of 10:1) in 10 μL PBS at 37 °C for 1 hr in the absence (lane 1) or presence of the indicated peptide/HSC73 mole ratio of NGT-Bw4 peptide (lanes 2–5) or NGT-Bw6 peptide (lanes 6–9). The mixtures were resolved by 7% native polyacrylamide gel electrophoresis (PAGE). Radiolabeled RCMLA was visualized by autoradiography of 125-Iodine. The slower-migrating bands correspond to HSC73-bound RCMLA.

competitive binding assay using RCMLA. RCMLA was labeled with 125-iodine, incubated with purified HSC73 in the absence or presence of various amounts of synthetic peptides and separated by a native PAGE. HSC73-bound RCMLA was detected as a slower migrating band (Fig. 6, lane 1). By increasing the amount of NGT-Bw4 peptide, levels of HSC73-bound RCMLA were decreased (Fig. 6, lanes 2–5). In contrast, less dissociation was observed in the addition of NGT-Bw6 peptide (Fig. 6, lanes 6–9). Thus, it was demonstrated that NGT-Bw4 and NGT-Bw6 have a high binding affinity and a low binding affinity to HSC73, respectively.

Analysis of TAP-dependent translocation of synthetic peptides

T1 cells and T2 cells were permeabilized by streptolysin-O and incubated with 125-iodine-labeled synthetic peptide, NGT-Bw4 or NGT-Bw6, at 37 °C in the presence of 1 mM ATP. Peptides translocated into the ER are glycosylated and, thus, can be collected by Con A Sepharose beads. The difference between radioactivities of the glycosylated peptide recovered from T1 cells and that from TAP-deficient T2 cells represents the TAP-dependent translocation level of the peptide. NGT-Bw4 was effectively translocated into the ER by TAP during a 20–60 min incubation (Fig. 7a). In contrast, NGT-Bw6 failed to be translocated by TAP (Fig. 7b).

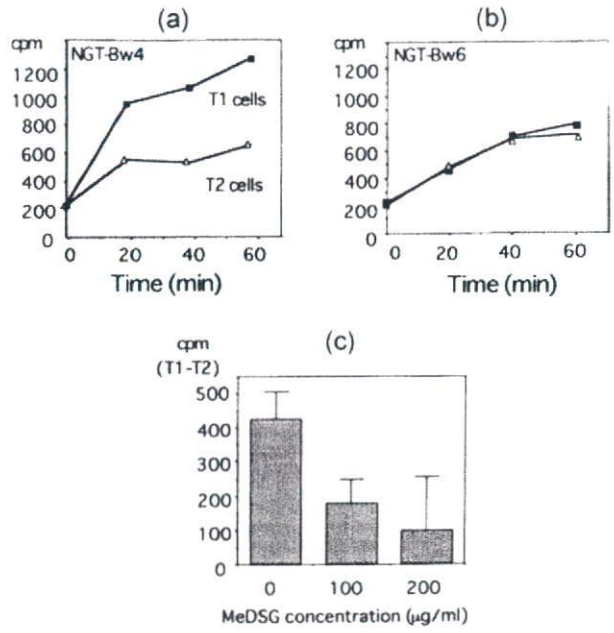

Fig. 7. ER translocation assay of synthetic peptides. 1×10^7 T1 cells or T2 cells were permeabilized by incubating with streptolysin-O as described earlier. Cells were then incubated with 19.0 μM 125-iodine-labeled peptides in the presence of 1 mM ATP. In the case of 0 min, non-permeabilized cells were incubated with the same amount of peptides. After the indicated time, glycosylated peptides were collected by Con A Sepharose beads, followed by counting radioactivity of the beads. (a) Time course of ER-translocation of NGT-Bw4 peptide in T1 cells (■) or T2 cells (△). (b) Time-course of ER-translocation of NGT-Bw6 peptide in T1 cells (■) or T2 cells (△). (c) Permeabilized T1 cells or T2 cells were incubated with radiolabeled NGT-Bw4 peptide in the transport buffer containing the indicated concentrations of MeDSG. Radioactivities of Con A Sepharose beads recovered from T2 cells were subtracted from those recovered from T1 cells, corresponding to TAP-dependent translocation levels. Bars represent SD from triplicated samples.

In order to determine if HSC73 is involved in the TAP-dependent translocation of NGT-Bw4 peptide, an ER translocation assay was performed in the absence or presence of 100 μg/mL or 200 μg/mL MeDSG, which induced the dissociation of HSC73 from TAP1. The TAP-dependent translocation of NGT-Bw4 was clearly inhibited by MeDSG in the presence of MeDSG (Fig. 7c). These results indicate that HSC73-binding affinity may affect the efficiency of TAP-dependent translocation into the ER, at least for some peptides, and that the physical association between HSC73 and TAP1 is important for the TAP-dependent translocation of HSC73-bound peptides.

HSC73-binding affinity of a natural MHC class I peptide F4.2

As NGT-Bw4 and NGT-Bw6 are not natural antigenic peptides, we tested if an MHC class I-presentable

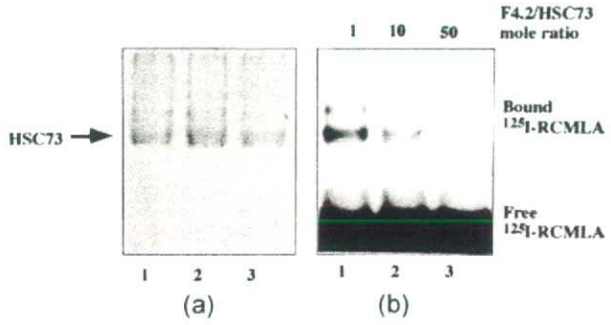

Fig. 8. HSC73-binding assay of antigenic peptide F4.2. RCMLA was labeled with 125-iodine by Iodo-beads as described earlier. Radiolabeled RCMLA (40 ng) was incubated with 2 μg HSC73 in a binding buffer at 37 °C for 1 hr in the presence of the indicated peptide/HSC73 mole ratio (lane 1, 1:1; lane 2, 10:1; lane 3, 50:1) of F4.2 peptide. The mixtures were resolved by 7% native polyacrylamide gel electrophoresis (PAGE). (a) HSC73 protein was visualized by staining the gel with Coomassie Brilliant Blue. The protein band corresponding to HSC73 is indicated. (b) Radiolabeled RCMLA was visualized by autoradiography of 125-iodine. The slower-migrating band observed at the position of HSC73 corresponds to HSC73-bound RCMLA.

natural peptide could bind to HSC73. By using acid elution and biochemical analyses, the structure of natural antigenic peptide of gastric signet ring cell carcinoma cells, HST-2, was determined (32). The peptide, named F4.2, is recognized by autologous cytotoxic T-cell clone TcHST-2 in the context of HLA-A31 restriction. F4.2 peptide was synthesized and incubated with 125-I-labeled RCMLA-HSC73 complex. After native PAGE separation, radioactivity was detected at the position of HSC73 (Fig. 8a), representing HSC73-bound RCMLA. Levels of the HSC73-bound RCMLA were decreased by increasing the amount of F4.2 peptide (Fig. 8b). Therefore, it was shown that the natural antigenic peptide F4.2 could bind to HSC73.

Cytosolic F4.2 peptide can be presented by HLA-A31

TcHST-2 cells are capable of responding to pulsed F4.2 peptide in a highly sensitive TNF production assay (32). In addition, we have shown that TcHST-2 also responds to the endogenous form of F4.2 peptide expressed by transfection of minigene vector pF4.2ss encoding the signal sequence plus F4.2 peptide (Fig. 9a). F4.2 peptide expressed by the minigene pF4.2ss can be translocated into the ER through the translocon protein by the signal peptide. Using a TNF production assay, we tested if TcHST-2 could respond to cytosolic F4.2 peptide expressed by transfection of minigene pF4.2 encoding just F4.2 peptide without the signal peptide (Fig. 9a). pF4.2reverse was constructed by insertion of the F4.2-coding oligonucleotides into the expression vector in an antisense orientation. Expression vectors were transfected to HOBC8-A31-12 cells, which express HLA-A31, followed by co-culture with TcHST-2 cells and TNF production assay. As shown in Figure 9b, pF4.2-transfected cells, as well as pF4.2ss-transfected cells, were recognized by TcHST-2 cells, whereas pF4.2reverse-transfected cells were not. These results indicate that cytosolic F4.2 without the signal peptide can be translocated into the ER through TAP.

Presentation of cytosolic F4.2 is inhibited by MeDSG treatment

In order to elucidate the involvement of HSC73 in the TAP-dependent translocation of F4.2 peptide, we tested the effect of MeDSG on the presentation of endogenous F4.2 peptide. C1R-A31 cells were transfected with either pF4.2 or pF4.2ss minigene expression vector and cultured in the absence or presence of 200 μg/mL MeDSG. Forty-eight hours after the transfection, cytotoxicity by TcHST-2 was examined by ^{51}Cr release assay. HST-2 cells and K562 cells were used as positive control target cells and negative control target cells, respectively (Fig. 9c, bars 1,2). Both pF4.2-transfected cells and pF4.2ss-transfected cells were lysed by TcHST-2 similarly. In the presence of MeDSG, however, only pF4.2ss-transfected cells were susceptible to killing by TcHST-2 (Fig. 9c, bars 5,7). Taken together with the result showing that HSC73 binds to F4.2, it is indicated that MeDSG-induced disruption of the HSC73-TAP complex results in the incomplete ER-translocation of the HSC73-bound antigenic peptide. Furthermore, our data imply that MeDSG may not affect the signal peptide-mediated translocation of antigenic peptides.

DISCUSSION

It has been speculated so far that HSP70 might be involved in antigen presentation. This idea came from evidence produced by us or other groups showing that: (i) MHC class I-bound antigenic peptide with an N-terminal short flanking sequence, which might be a cytoplasmic precursor of the antigenic peptide, was isolated from murine tumor cell lysates as a HSP70-binding peptide (18); (ii) HSP70 could bind to some antigenic peptides and present them to T cells (18, 20, 46); and (iii) the vaccination of HSP70 plus tumor-derived peptides could enhance the anti-tumor immunity in animals (47–50). Moreover, there are some reports demonstrating the involvement of HSP70 in the TAP-independent presentation of cytosolic antigens and in the MHC class II antigen presentation (51, 52). In our experiments, it was revealed that HSC73, the constitutively expressed HSP70 family protein, was associated with TAP1 in an ATP-dependent manner, which was consistent with the report of Chen and Androlewicz (53).

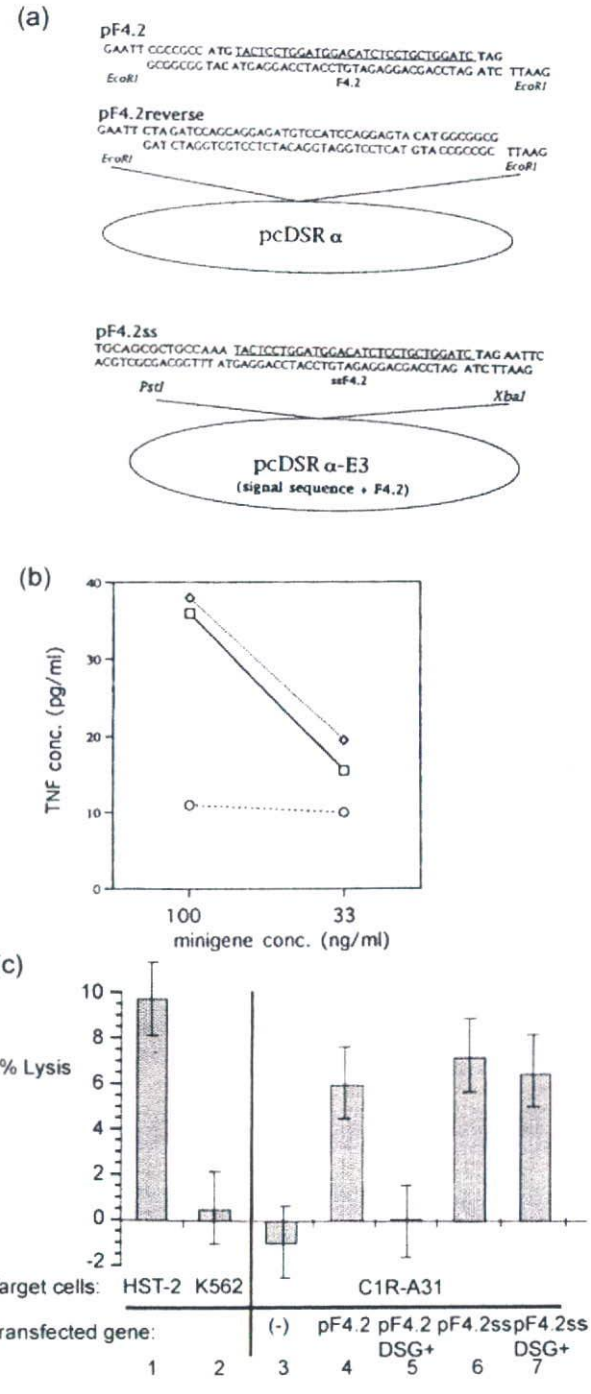

Fig. 9. T-cell recognition of gene-transferred F4.2 peptide and the effect of MeDSG. (a) Construction and nucleotide sequence of minigene vectors. Construction and nucleotide sequence (underline) of pF4.2, pF4.2reverse and pF4.2ss minigene vectors are illustrated. pF4.2 and pF4.2reverse were constructed by insertion of the F4.2-coding oligonucleotides into the *Eco*RI site of the pcDSRα expression vector in a sense orientation or an antisense orientation, respectively. pF4.2ss was constructed by insertion of F4.2-coding oligonucleotides into the *Pst*I and *Xba*I sites of the pcDSRα-E3 expression vector containing an adenovirus E3/19 kDa protein signal sequence. (b) Cytosolic F4.2 peptide can be presented by HLA-A31. HOBC8-A31-12 cells that express HLA-A31 were transfected with 100 ng/mL or 33 ng/mL pF4.2, pF4.2reverse or pF4.2ss. Forty-eight hours after the transfection, cells were incubated with TcHST-2 for 10 hr at an E/T ratio of 3:1 and then tumor necrosis factor (TNF) production was determined. □, pF4.2ss; △, pF4.2; , pF4.2reverse. (c) Effect of MeDSG on the cytotoxic susceptibility ofminigene-transfected cells by TcHST-2. C1R-A31 cells that express HLA-A31 were transfected with 100 ng/mL pF4.2 or pF4.2ss minigene expression vector by Lipofectin reagent and cultured in the absence (bars 4, 6) or presence of 200 μg/mL MeDSG (bars 5, 7) for 48 hr. Then, HST-2 cells (bar 1), K562 cells (bar 2) and C1R-A31 cells without (bar 3) or with minigene transfection (bars 4–7) were labeled with ^{51}Cr and were mixed with TcHST-2 for 10 hr at an E/T ratio of 10:1, followed by counting radioactivities of ^{51}Cr in the culture supernatants. Error bars represent SD calculated from triplicated samples

HSC73 is a cytosolic protein functioning as a molecular chaperone (54). It has a peptide binding domain in the C-terminal region, which has a high affinity to peptides containing several hydrophobic amino acids (55). Isolation and sequencing of MHC class I-bound antigenic peptides revealed that most of the peptides contain hydrophobic amino acids, some of which are important as anchor residues to the groove formed on the MHC class I molecule. The hydrophobic peptides become solubilized by binding to chaperone proteins such as heat shock proteins. In addition, chaperone-bound peptides may be protected from degradation by cytosolic peptidases. In the ER, antigenic peptides are transferred from TAP to MHC class I molecule through tapasin-mediated interaction between these two molecules (9, 11). It has been reported so far that molecular chaperones such as gp96 and calreticulin bind to antigenic peptides in the ER and may mediate their transfer from TAP to MHC class I heavy chain (17, 56). In contrast to the event in the ER, less is known about the feeding mechanism of cytoplasmic peptides to TAP. We tried to detect a physical interaction between TAP and proteasome; however we failed (unpublished data). Thus, it is possible that antigenic peptides produced by proteasomes in the cytosol could be carried to TAP by some cytosolic chaperones such as HSC73 and HSP90. Actually, evidence has been reported that N-terminally extended peptides are associated with the cytosolic chaperone, TriC, and are protected from degradation by cytosolic peptidases (57). In addition, Yamano *et al.* provided evidence that HSP90 and PA28 accelerated the processing and presentation of MHC class I-bound peptides (58).

In order to determine the functional significance of the interaction between HSC73 and TAP1, we used an immunosuppressant, MeDSG, a stable analog of 15-DSG, which could specifically bind to HSC73 (29, 59). Treatment of T1 cells with MeDSG resulted in the

downregulation of the cell surface levels of MHC class I expression. The downregulatory effect of MeDSG was specific in the expression of MHC class I, as other surface molecules such as CD3 and LFA-1 were not changed by treatment of cells with the same concentration of MeDSG (data not shown). These data are consistent with a previous report showing a decreased expression of MHC class I by 15-DSG in a rat allograft model and cultured mouse cells (23, 42). The decreased MHC class I levels of T1 cells after MeDSG treatment were very similar to the levels of T2 cells, which lacked TAP molecules. MHC class I becomes unstable and the cell surface levels are decreased if TAP-dependent translocation of antigenic peptides is impaired (4). Therefore, it was suggested that MeDSG might inhibit antigen presentation at the TAP level.

15-DSG binds to both HSC73 and HSP90. Based on previous reports, there may be two 15-DSG-binding regions in HSC73 (60). One resides in the ATP-binding region and the other is the C-terminus EEVD domain, which is conserved among HSP70-family proteins. HSP90 also contains the same sequence in its C-terminus. Previously, Nadler *et al.* demonstrated that 15-DSG could inhibit the nuclear translocation of transcriptional factor nuclear factor-kappa B (NF-κB) by competitively blocking the association of HSC73 with NF-κB (59). This was the first report elucidating the molecular mechanism of immunosuppression by 15-DSG. In the present study, we showed evidence that MeDSG could not affect the interaction between HSC73 and a substrate protein. Although MeDSG contains a spermidine-like structure, it is known that spermidine had low affinity to HSC73 and less immunosuppressive activity (43). We confirmed that spermidine could neither downregulate the MHC class I expression in T1 cells (data not shown) nor inhibit the interaction between HSC73 and TAP1. However, it cannot be ruled out that the inhibitory effect of MeDSG to antigen presentation might be mediated by binding of MeDSG to HSP90, as it is definitive that HSP90 also serves as a chaperone for antigenic peptides in the cytosol (58, 61). Therefore, we then executed an ER-translocation study using two model peptides that have distinct binding affinity to HSC73. HSC73-bound peptide NGT-Bw4 could be translocated by TAP, whereas low-affinity peptide NGT-Bw6 failed. As amino acid sequences of these peptides are highly homologous and are identical, especially at their N-terminal and C-terminal residues which are known to affect the binding affinity to TAP (62), it is likely that the difference in the TAP-mediated translocation results from the distinct binding affinity to HSC73. Taken together, it is indicated that MeDSG could dissociate HSC73 from TAP, leading to a decrease of TAP-dependent translocation of HSC73-chaperoned peptides.

To confirm further that MeDSG inhibits the MHC class I antigen presentation, we performed experiments using a natural antigenic peptide, F4.2, which was identified from human gastric cancer cell line HST-2 (32). F4.2 is presented by HLA-A31 and recognized by cytotoxic T-cell clone, TcHST-2. We found that F4.2 peptide had high affinity to HSC73. By using minigenes coding F4.2, it was shown that the presentation of the cytosolic peptide chaperoned by HSC73 was inhibited by MeDSG. In contrast, TAP-independent presentation of F4.2 peptide, possibly through translocon, was not affected by MeDSG. However, it cannot be ruled out that HSC73 might function as a molecular chaperone for TAP itself and, therefore, MeDSG might disturb the structure and function of TAP.

Meanwhile, it is considered that the repertoire of MHC class I peptides could be affected by: (i) the MHC class I binding motif; (ii) the binding affinity to TAP; and (iii) the proteasomal cleavage site of antigenic proteins. Our data proposed another possibility that the HSC73-binding affinity might also affect the repertoire of MHC class I peptides. Our findings are likely to be important in the field of tumor immunotherapy, especially in the design of antigenic peptides for developing peptide vaccines. There is much evidence that CTL fail to kill tumor cells even though they are successfully induced by pulsing synthetic peptides to antigen-presenting cells. It is possible that some peptides might not be translocated into the ER if the peptides have low HSC73-binding affinity, as in the case of NGT-Bw6. As discussed previously, there are multiple cytosolic chaperones for antigenic peptides, such as TriC, HSP90, PA28 and HSC73, each of which is involved in the processing and transportation of antigenic peptides independently or cooperatively (57, 58, 61). Therefore, HSC73-binding affinity of the peptides and the proper function of HSC73 is not the only factor limiting the peptide presentation.

Our data showing the ATP-dependent dissociation of HSC73 from TAP1 present some important implications for the molecular machinery of the peptide-feeding mechanism to TAP. HSC73 has an ATP-binding domain in the N-terminal region and an intrinsic ATPase activity. It is known that the ADP-binding form of HSC73 has a higher affinity to hydrophobic peptides than the ATP-binding form (63). The contact of empty (peptide-free) HSC73 to peptides can stimulate the intrinsic ATPase activity of HSC73, resulting in the formation of a stable ADP-HSC73-peptide complex (64). In the presence of ATP, HSC73-bound ADP is exchanged to ATP, and the peptide is released from the ATP-binding HSC73 (65). Thus, HSC73 has an association/dissociation cycle with a substrate peptide depending upon the presence of ATP and the intrinsic ATPase activity. As the ADP-binding form

of HSC73, which carries a peptide, has higher affinity to TAP than the ATP-binding form, the HSC73-bound antigenic peptide can be brought to close proximity to TAP. It is reported that DSG binds to HSC73 in its C-terminal EEVD domain, which could affect the conformation of the ATP-binding domain (59, 66). Therefore, HSC73 might interact with TAP by the same domain, leading to ADP-ATP exchange. In the presence of ATP, peptides can be released from HSC73, resulting in the transfer of peptides to TAP. Following the ATP-dependent feeding of the peptides, ATP-binding HSC73 (empty form) may be dissociated from TAP to bind to other peptides. It is possible that HSC73 may feed the cytosolic antigenic peptides by such an ATP-dependent cycle.

Where and how can HSC73 catch antigenic peptides produced by proteasome? In this context, it is of interest to test whether ATP-binding HSC73 is associated with proteasome. Further experiments focusing on the interaction between proteasome and chaperone will clarify the molecular machinery of antigenic peptide transportation in the cytoplasm.

Q8

ACKNOWLEDGMENTS

We thank Dr Peter Cresswell (Yale University, New Haven, CT, USA) for providing us with the affinity purified polyclonal anti-TAP1 antibody, R.RING4C and Dr Hisakazu Nemoto (Nippon Kayaku, Tokyo, Japan) for providing us with MeDSG. Recombinant interleukin-2 was kindly provided by Shionogi Pharmaceutical Co. Ltd, Osaka, Japan. Genomic HLA-A*31012 DNA was kindly provided by Dr M. Takiguchi of Kumamoto University School of Medicine, Kumamoto, Japan. HOBC8 was kindly provided by Dr P. Coulie of Ludwig Institute for Cancer Research, Brussels, Belgium. pcDSRα-E3 was kindly provided by Dr E. De Plaen and Dr P. Chomez of Ludwig Institute for Cancer Research, Brussels, Belgium and Dr J. R. Miller at DNAX Research Institute of Molecular and Cellular Biology, Palo Alto, CA, USA. We also thank Dr. Keiji Tanaka (Tokyo Metropolitan Research Institute, Tokyo, Japan) for helpful discussion. This work was supported by a Grant-in-Aid for Scientific Research from the Ministry of Education, Culture and Science of Japan and from the Akiyama Foundation.

REFERENCES

1. Michalek M.T., Grant E.P., Gramm C., Goldberg A.L., Rock K.L. (1993) A role for the ubiquitin-dependent proteolytic pathway in MHC class I-restricted antigen presentation. *Nature* **363:** 552–4.
2. Kelly A., Powis S.H., Kerr L.A., Mockridge I., Elliott T., Bastin J., Uchanska Ziegler B., Ziegler A., Trowsdale J., Townsend A. (1992) Assembly and function of the two ABC transporter proteins encoded in the human major histocompatibility complex. *Nature* **355:** 641–4.
3. Powis S.J., Townsend A.R., Deverson E.V., Bastin J., Butcher G.W., Howard J.C. (1991) Restoration of antigen presentation to the mutant cell line RMA-S by an MHC-linked transporter. *Nature* **354:** 528–31.
4. Spies T., Cerundolo V., Colonna M., Cresswell P., Townsend A., DeMars R. (1992) Presentation of viral antigen by MHC class I molecules is dependent on a putative peptide transporter heterodimer. *Nature* **355:** 644–6.
5. Neefjes J.J., Momburg F., Hammerling G.J. (1993) Selective and ATP-dependent translocation of peptides by the MHC-encoded transporter [published erratum appears in Science 1994 Apr 1;264(5155):16]. *Science* **261:** 769–71.
6. Shepherd J.C., Schumacher T.N., Ashton Rickardt P.G., Imaeda S., Ploegh H.L., Janeway C.A. Jr., Tonegawa S. (1993) TAP1-dependent peptide translocation in vitro is ATP dependent and peptide selective [published erratum appears in Cell 1993 Nov 19;75(4):613]. *Cell* **74:** 577–84.
7. Androlewicz M.J., Ortmann B., van Endert P.M., Spies T., Cresswell P. (1994) Characteristics of peptide and major histocompatibility complex class I/beta 2-microglobulin binding to the transporters associated with antigen processing (TAP1 and TAP2). *Proc Natl Acad Sci USA* **91:** 12716–20.
8. Grandea A.G.r., Androlewicz M.J., Athwal R.S., Geraghty D.E., Spies T. (1995) Dependence of peptide binding by MHC class I molecules on their interaction with TAP. *Science* **270:** 105–8.
9. Ortmann B., Androlewicz M.J., Cresswell P. (1994) MHC class I/beta 2-microglobulin complexes associate with TAP transporters before peptide binding. *Nature* **368:** 864–7.
10. Sadasivan B., Lehner P.J., Ortmann B., Spies T., Cresswell P. (1996) Roles for calreticulin and a novel glycoprotein, tapasin, in the interaction of MHC class I molecules with TAP. *Immunity* **5:** 103–14.
11. Suh W.K., Cohen Doyle M.F., Fruh K., Wang K., Peterson P.A., Williams D.B. (1994) Interaction of MHC class I molecules with the transporter associated with antigen processing. *Science* **264:** 1322–6.
12. Ortmann B., Copeman J., Lehner P.J., Sadasivan B., Herberg J.A., Grandea A.G., Riddell S.R., Tampe R., Spies T., Trowsdale J., Cresswell P. (1997) A critical role for tapasin in the assembly and function of multimeric MHC class I-TAP complexes. *Science* **277:** 1306–9.
13. Nair S., Wearsch P.A., Mitchell D.A., Wassenberg J.J., Gilboa E., Nicchitta C.V. (1999) Calreticulin displays in vivo peptide-binding activity and can elicit CTL responses against bound peptides. *J Immunol* **162:** 6426–32.
14. Lindquist J.A., Jensen O.N., Mann M., Hammerling G.J. (1998) ER-60, a chaperone with thiol-dependent reductase activity involved in MHC class I assembly. *Embo J* **17:** 2186–95.
15. Morrice N.A., Powis S.J. (1998) A role for the thiol-dependent reductase ERp57 in the assembly of MHC class I molecules. *Curr Biol* **8:** 713–6.
16. Srivastava P.K., Udono H. (1994) Heat shock protein-peptide complexes in cancer immunotherapy. *Curr Opin Immunol* **6:** 728–32.
17. Srivastava P.K., Udono H., Blachere N.E., Li Z. (1994) Heat shock proteins transfer peptides during antigen processing and CTL priming. *Immunogenetics* **39:** 93–8.
18. Ishii T., Udono H., Yamano T., Ohta H., Uenaka A., Ono T., Hizuta A., Tanaka N., Srivastava P.K., Nakayama E. (1999) Isolation of MHC class I-restricted tumor antigen peptide and its precursors associated with heat shock proteins hsp70, hsp90, and gp96. *J Immunol* **162:** 1303–9.

19. Kishi A., Ichinohe T., Hirai I., Kamiguchi K., Tamura Y., Kinebuchi M., Torigoe T., Ichimiya S., Kondo N., Ishitani K., Yoshikawa T., Kondo M., Matsuura A., Sato N. (2001) The cell surface-expressed HSC70-like molecule preferentially reacts with the rat T-cell receptor Vdelta6 family. *Immunogenetics* **53:** 401–9.
20. Takashima S., Sato N., Kishi A., Tamura Y., Hirai I., Torigoe T., Yagihashi A., Takahashi S., Sagae S., Kudo R., Kikuchi K. (1996) Involvement of peptide antigens in the cytotoxicity between 70-kDa heat shock cognate protein-like molecule and CD3+, CD4−, CD8−, TCR-alpha beta- killer T cells. *J Immunol* **157:** 3391–5.
21. Tamura Y., Tsuboi N., Sato N., Kikuchi K. (1993) 70 kDa heat shock cognate protein is a transformation-associated antigen and a possible target for the host's anti-tumor immunity. *J Immunol* **151:** 5516–24.
22. Udono H., Srivastava P.K. (1994) Comparison of tumor-specific immunogenicities of stress-induced proteins gp96, hsp90, and hsp70. *J Immunol* **152:** 5398–403.
23. Binder R.J., Blachere N.E., Srivastava P.K. (2001) Heat shock protein-chaperoned peptides but not free peptides introduced into the cytosol are presented efficiently by major histocompatibility complex I molecules. *J Biol Chem* **276:** 17 163–71.
24. Nihei T., Sato N., Takahashi S., Ishikawa M., Sagae S., Kudo R., Kikuchi K., Inoue A. (1993) Demonstration of selective protein complexes of p53 with 73 kDa heat shock cognate protein, but not with 72 kDa heat shock protein in human tumor cells. *Cancer Lett* **73:** 181–9.
25. Nihei T., Takahashi S., Sagae S., Sato N., Kikuchi K. (1993) Protein interaction of retinoblastoma gene product pRb110 with M(r) 73,000 heat shock cognate protein. *Cancer Res* **53:** 1702–5.
26. Inoue A., Torigoe T., Sogahata K., Kamiguchi K., Takahashi S., Sawada Y., Saijo M., Taya Y., Ishii S., Sato N. (1995) 70-kDa heat shock cognate protein interacts directly with the N-terminal region of the retinoblastoma gene product pRb. Identification of a novel region of pRb-mediating protein interaction. *J Biol Chem* **270:** 22 571–6.
27. Hartl F.U. (1991) Heat shock proteins in protein folding and membrane translocation. *Semin Immunol* **3:** 5–16.
28. Kawasaki C., Okamura S., Shimoda K., Nemoto K., Niho Y. (1995) In vitro study of deoxymethylspergualin on functions of lymphocytes and bone marrow cells from healthy volunteers. *J Antibiot Tokyo* **48:** 243–7.
29. Nadler S.G., Tepper M.A., Schacter B., Mazzucco C.E. (1992) Interaction of the immunosuppressant deoxyspergualin with a member of the Hsp70 family of heat shock proteins. *Science* **258:** 484–6.
30. Amemiya H., NKT-01, J.C.T.S.G.o. (1995) Immunosuppressive mechanisms and action of deoxyspergualin in experimental and clinical studies. *Transplant. Proceedings* **27:** 31–2.
31. Fujii H., Takada T., Nemoto K., Abe F., Fujii A., Talmadge J.E., Takeuchi T. (1992) Deoxyspergualin, a novel immunosuppressant, markedly inhibits human mixed lymphocyte reaction and cytotoxic T-lymphocyte activity in vitro. *Int J Immunopharmacol* **14:** 731–7.
32. Suzuki K., Sahara H., Okada Y., Yasoshima T., Hirohashi Y., Nabeta Y., Hirai I., Torigoe T., Takahashi S., Matsuura A., Takahashi N., Sasaki A., Suzuki M., Hamuro J., Ikeda H., Wada Y., Hirata K., Kikuchi K., Sato N. (1999) Identification of natural antigenic peptides of a human gastric signet ring cell carcinoma recognized by HLA-A31-restricted cytotoxic T lymphocytes. *J Immunol* **163:** 2783–91.
33. Hosken N.A., Bevan M.J. (1990) Defective presentation of endogenous antigen by a cell line expressing class I molecules. *Science* **248:** 367–70.
34. Yasoshima T., Sato N., Hirata K., Kikuchi K. (1995) The mechanism of human autologous gastric signet ring cell tumor rejection by cytotoxic T lymphocytes in the possible context of HLA-A31 molecule. *Cancer* **75:** 1484–9.
35. Nossner E., Goldberg J.E., Naftzger C., Lyu S.C., Clayberger C., Krensky A.M. (1996) HLA-derived peptides which inhibit T cell function bind to members of the heat-shock protein 70 family. *J Exp Med* **183:** 339–48.
36. Fourie A.M., Sambrook J.F., Gething M.J. (1994) Common and divergent peptide binding specificities of hsp70 molecular chaperones. *J Biol Chem* **269:** 30 470–8.
37. Androlewicz M.J., Anderson K.S., Cresswell P. (1993) Evidence that transporters associated with antigen processing translocate a major histocompatibility complex class I-binding peptide into the endoplasmic reticulum in an ATP-dependent manner. *Proc Natl Acad Sci USA* **90:** 9130–4.
38. Anderson K., Cresswell P., Gammon M., Hermes J., Williamson A., Zweerink H. (1991) Endogenously synthesized peptide with an endoplasmic reticulum signal sequence sensitizes antigen processing mutant cells to class I- restricted cell-mediated lysis. *J Exp Med* **174:** 489–92.
39. Brot N., Redfield B., Qiu N.H., Chen G.J., Vidal V., Carlino A., Weissbach H. (1994) Similarity of nucleotide interactions of BiP and GTP-binding proteins. *Proc Natl Acad Sci USA* **91:** 12 120–4.
40. Hoeger P.H., Tepper M.A., Faith A., Higgins J.A., Lamb J.R., Geha R.S. (1994) Immunosuppressant deoxyspergualin inhibits antigen processing in monocytes. *J Immunol* **153:** 3908–16.
41. Takasu S., Sakagami K., Morisaki F., Kawamura T., Haisa M., Oiwa T., Inagaki M., Hasuoka H., Kurozumi Y., Orita K. (1991) Immunosuppressive mechanism of 15-deoxyspergualin on sinusoidal lining cells in swine liver transplantation: suppression of MHC class II antigens and interleukin-1 production. *J Surgical Res* **51:** 165–9.
42. Waaga A.M., Ulrichs K., Krzymanski M., Treumer J., Hansmann M.L., Rommel T., Muller-Ruchholtz W. (1990) The immunosuppressive agent 15-deoxyspergualin induces tolerance and modulates MHC-antigen expression and interleukin-1 production in the early phase of rat allograft responses. *Transplant Proceedings* **22:** 1613–4.
43. Nadeau K., Nadler S.G., Saulnier M., Tepper M.A., Walsh C.T. (1994) Quantitation of the interaction of the immunosuppressant deoxyspergualin and analogs with Hsc70 and Hsp90. *Biochemistry* **33:** 2561–7.
44. Fujii H., Takada T., Nemoto K., Abe F., Takeuchi T. (1989) Stability and immunosuppressive activity of deoxyspergualin in comparison with deoxymethylspergualin. *Transplant Proc* **21:** 3471–3.
45. Maeda H., Sahara H., Mori Y., Torigoe T., Kamiguchi K., Tamura Y., Hirata K., Sato N. (2007) Biological heterogeneity of the peptide-binding motif of the 70-kDa heat shock protein by surface plasmon resonance analysis. *J Biol Chem* **282:** 26 956–62.
46. Blachere N.E., Li Z., Chandawarkar R.Y., Suto R., Jaikaria N.S., Basu S., Udono H., Srivastava P.K. (1997) Heat shock protein-peptide complexes, reconstituted in vitro, elicit peptide-specific cytotoxic T lymphocyte response and tumor immunity. *J Exp Med* **186:** 1315–22.
47. Bendz H., Ruhland S.C., Pandya M.P., Hainzl O., Riegelsberger S., Brauchle C., Mayer M.P., Buchner J., Issels R.D., Noessner E. (2007) Human heat shock protein 70 enhances tumor antigen presentation through complex formation and intracellular antigen delivery without innate immune signaling. *J Biol Chem.*
48. Kammerer R., Stober D., Riedl P., Oehninger C., Schirmbeck R., Reimann J. (2002) Noncovalent association with stress protein facilitates cross-priming of CD8+ T cells to tumor cell antigens by dendritic cells. *J Immunol* **168:** 108–17.

Q9

Q10

49. Tamura Y., Peng P., Liu K., Daou M., Srivastava P.K. (1997) Immunotherapy of tumors with autologous tumor-derived heat shock protein preparations. *Science* **278:** 117–20.
50. Ueda G., Tamura Y., Hirai I., Kamiguchi K., Ichimiya S., Torigoe T., Hiratsuka H., Sunakawa H., Sato N. (2004) Tumor-derived heat shock protein 70-pulsed dendritic cells elicit tumor-specific cytotoxic T lymphocytes (CTLs) and tumor immunity. *Cancer Sci* **95:** 248–53.
51. Panjwani N., Akbari O., Garcia S., Brazil M., Stockinger B. (1999) The HSC73 molecular chaperone: involvement in MHC class II antigen presentation. *J Immunol* **163:** 1936–42.
52. Schirmbeck R., Bohm W., Reimann J. (1997) Stress protein (hsp73)-mediated, TAP-independent processing of endogenous, truncated SV40 large T antigen for Db-restricted peptide presentation. *Eur J Immunol* **27:** 2016–23.
53. Chen D., Androlewicz M.J. (2001) Heat shock protein 70 moderately enhances peptide binding and transport by the transporter associated with antigen processing. *Immunol Lett* **75:** 143–8.
54. Rassow J., Voos W., Pfanner N. (1995) Partner proteins determine multiple functions of Hsp70. *Trends in Cell Biol* **5:** 207–12.
55. Gierasch L.M. (1994) Molecular chaperones. Panning for chaperone-binding peptides. *Curr Biol* **4:** 173–4.
56. Basu S., Srivastava P.K. (1999) Calreticulin, a peptide-binding chaperone of the endoplasmic reticulum, elicits tumor- and peptide-specific immunity. *J Exp Med* **189:** 797–802.
57. Kunisawa J., Shastri N. (2003) The group II chaperonin TRiC protects proteolytic intermediates from degradation in the MHC class I antigen processing pathway. *Mol Cell* **12:** 565–76.
58. Yamano T., Murata S., Shimbara N., Tanaka N., Chiba T., Tanaka K., Yui K., Udono H. (2002) Two distinct pathways mediated by PA28 and hsp90 in major histocompatibility complex class I antigen processing. *J Exp Med* **196:** 185–96.
59. Nadler S.G., Eversole A.C., Tepper M.A., Cleaveland J.S. (1995) Elucidating the mechanism of action of the immunosuppressant 15-deoxyspergualin. *Ther Drug Monit* **17:** 700–3.
60. Nadler S.G., Dischino D.D., Malacko A.R., Cleaveland J.S., Fujihara S.M., Marquardt H. (1998) Identification of a binding site on Hsc70 for the immunosuppressant 15- deoxyspergualin. *Biochem Biophys Res Commun* **253:** 176–80.
61. Kunisawa J., Shastri N. (2006) Hsp90alpha chaperones large C-terminally extended proteolytic intermediates in the MHC class I antigen processing pathway. *Immunity* **24:** 523–34.
62. Uebel S., Kraas W., Kienle S., Wiesmuller K.-H., Jung G., Tampe R. (1997) Recognition principle of the TAP-transporter disclosed by combinatorial peptide libraries. *Proc Natl Acad Sci USA* **94:** 8976–81.
63. Beckmann R.P., Mizzen L.E., Welch W.J. (1990) Interaction of Hsp 70 with newly synthesized proteins: implications for protein folding and assembly. *Science* **248:** 850–54.
64. Jordan R., McMacken R. (1995) Modulation of the ATPase activity of the molecular chaperone DnaK by peptides and the DnaJ and GrpE heat shock proteins. *J Biol Chem* **270:** 4563–9.
65. Szabo A., Langer T., Schroder H., Flanagan J., Bukau B., Hartl F.U. (1994) The ATP hydrolysis-dependent reaction cycle of the Escherichia coli Hsp70 system-DnaK, DnaJ, and GrpE. *Proc Natl Acad Sci USA* **91:** 10 345–9.
66. Freeman B.C., Myers M.P., Schumacher R., Morimoto R.I. (1995) Identification of a regulatory motif in Hsp70 that affects ATPase activity, substrate binding and interaction with HDJ-1. *Embo J* **14:** 2281–92.

Prognostic impact and immunogenicity of a novel osteosarcoma antigen, papillomavirus binding factor, in patients with osteosarcoma

Tomohide Tsukahara,[1,2,3] Satoshi Kawaguchi,[2,5] Toshihiko Torigoe,[3] Shigeharu Kimura,[3] Masaki Murase,[2,3] Shingo Ichimiya,[3] Takuro Wada,[2] Mitsunori Kaya,[2] Satoshi Nagoya,[2] Takeshi Ishii,[4] Shin-ichiro Tatezaki,[4] Toshihiko Yamashita[2] and Noriyuki Sato[3]

[1]Research Fellow of the Japan Society for the Promotion of Science, [2]Department of Orthopaedic Surgery, Sapporo Medical University School of Medicine, South-1, West-16, Chuo-ku, Sapporo, 060-8543; [3]Department of Pathology, Sapporo Medical University School of Medicine, South-1, West-17, Chuo-ku, Sapporo, 060-8556; [4]Division of Orthopaedic Surgery, Chiba Cancer Center, 666-2 Nitona-cho, Chuo-ku, Chiba, 260-8717, Japan

(Received October 10, 2007/Accepted October 28, 2007/Online publication February 4, 2008)

To develop peptide-based immunotherapy for osteosarcoma, we previously identified papillomavirus binding factor (PBF) as a cytotoxic T lymphocytes (CTL)-defined osteosarcoma antigen in the context of human leukocyte antigen (HLA)-B55. In the present study, we analyzed the distribution profile of PBF in 83 biopsy specimens of osteosarcomas and also the prognostic impact of PBF expression in 78 patients with osteosarcoma who had completed the standard treatment protocols. Next, we determined the antigenic peptides from PBF that react with peripheral T lymphocytes of HLA-A24$^+$ patients with osteosarcoma. Immunohistochemical analysis revealed that 92% of biopsy specimens of osteosarcoma expressed PBF. PBF-positive osteosarcoma conferred significantly poorer prognosis than those with negative expression of PBF ($P = 0.025$). In accordance with the Bioinformatics and Molecular Analysis Section score, we synthesized 10 peptides from the PBF sequence. Subsequent screening with an HLA class I stabilization assay revealed that peptide PBF A24.2 had the highest affinity to HLA-A24. CD8$^+$ T cells reacting with a PBF A24.2 peptide were detected in eight of nine HLA-A24-positive patients with osteosarcoma at the frequency from 5×10^{-7} to 7×10^{-6} using limiting dilution/mixed lymphocyte peptide culture followed by tetramer-based frequency analysis. PBF A24.2 peptide induced CTL lines from an HLA-A24-positive patient, which specifically killed an osteosarcoma cell line that expresses both PBF and HLA-A24. These findings suggested prognostic significance and immunodominancy of PBF in patients with osteosarcoma. PBF is the candidate target for immunotherapy in patients with osteosarcoma. (*Cancer Sci* 2008; 99: 368–375)

Osteosarcoma is the most common primary malignant tumor of bone. The past three decades have witnessed remarkable advances in the treatment of osteosarcoma. These include the introduction of adjuvant chemotherapy, establishment of guidelines for adequate surgical margins, and the development of postexcision reconstruction.[1,2] There have also been advances in the field of immunotherapy for osteosarcoma that, unfortunately, have received less attention.[3,4] However, the current stagnation in chemotherapy-based treatments for osteosarcoma has reignited interest in immunotherapeutic approaches.[5,6]

Recent immunotherapy depends largely on understanding of the molecular interactions between T cell receptors (TCR) on cytotoxic T lymphocytes (CTL) and antigenic peptides on tumor cells. This has led to a variety of vaccination approaches, including those with antigenic peptides[7] recombinant viruses encoding antigenic genes[8] dendritic cells[9] and T lymphocytes, in which the TCR recognizing an antigenic peptide is genetically engineered.[10] Nevertheless, such immunotherapeutic approaches were hampered in osteosarcoma by a lack of defined antigens until we recently identified papillomavirus binding factor (PBF) using an osteosarcoma cell line and an autologous CTL clone restricted by human leukocyte antigen (HLA)-B*5502.[11,12] PBF is a DNA-binding transcription factor with unknown function.[13,14] The oncogenic role of PBF in osteosarcoma and its immunogenicity in patients with common HLA alleles such as HLA-A2 and HLA-A24 needs to be disclosed before development of clinically applicable PBF-based immunotherapy.

In the present study, we analyzed the distribution profile, prognostic impact, and immunogenicity of PBF in patients with osteosarcoma. Immunogenicity analysis focused on frequency and cytotoxicity of T cells in patients with HLA-A24 allele by using limiting dilution (LD)/mixed lymphocyte peptide culture (MLPC)/tetramer assays.

Materials and Methods

This study was approved under institutional guidelines for the use of human subjects in research. The patients and their families as well as healthy donors gave informed consent for the use of blood samples and tissue specimens in our research.

Generation of anti-PBF antibody. A polyclonal antibody against PBF was generated by immunizing rabbits with 100 μg of a 15-mer peptide, CGDTVDSDQFKREED, once per week for six weeks (SigmaGenosys, Sapporo, Japan). The serum was collected seven days after the last immunization and purified using Protein A column. The specificity of the anti-PBF antibody was confirmed previously by Western blotting and immunostaining.[12]

Immunohistochemistry. Formalin-fixed paraffin-embedded sections were obtained from 83 biopsy specimens of the primary lesion of osteosarcoma (Table 1). The sections were deparaffinized, boiled in a microwave oven, and blocked with 1% non-fat dry milk before staining with streptavidin-biotin-complex (Nichirei, Tokyo, Japan) as previously described.[15] Hematoxylin was used for counter staining. The reactivity of the anti-PBF antibody was determined by staining of the nuclei of tumor cells.[12] The expression status of PBF was graded semiquantitatively according to the modified classification described by Al-Batran *et al.*[16,17] negative (positive cells <5%), low (≤5% positive cells ≤50%), and high (positive cells >50%) (Fig. 1). Diffuse expression and heterogeneous expression were regarded as high grade and low grade, respectively. Focal expression was graded as low or negative according to the percentage of positive cells.

[5]To whom correspondence should be addressed. E-mail: kawaguch@sapmed.ac.jp
Grant support: This work was supported by Grants-in-Aid from the Ministry of Education, Culture, Sports, Science and Technology of Japan (Grant no. 16209013 to N. Sato), Practical Application Research from the Japan Science and Technology Agency (Grant No. H14-2 to N. Sato), the Ministry of Health, Labor and Welfare (Grant No. H17-Gann-Rinsyo-006 to T. Wada), Postdoctoral Fellowship of the Japan Society for the Promotion of Science (Grant no. 02568 to T. Tsukahara) and Northern Advancement Center for Science and Technology (Grant No. H18-Waka-075 to T. Tsukahara).

doi: 10.1111/j.1349-7006.2008.00695.x

Table 1. The grade of PBF expressioni and the progonosis in 83 patients with osteosarcoma

Patients	Age	Gender	Location	Surgical stage	Histological type	Chemotherapy	Histological response grade	Operation	PBF expression	EFS (months)	OS (months)	Prognosis
1	15	M	Femur	IIB	Osteoblastic	T-12	2	Amputation	High	39	46	DOD
2	20	M	Humerus	IIB	Osteoblastic	T-12	0	Amputation	Low	12	24	DOD
3	9	F	Femur	IIB	Chondroblastic	T-12	0	WE+FVFG	High	14	22	DOD
4	12	M	Femur	IIB	Osteoblastic	T-12	0	Amputation	Low	3	9	DOD
5	10	F	Humerus	IIB	Teleangiectatic	T-12	1	WE+FVFG	High	103	103	CDF
6	17	F	Humerus	IIB	Osteoblastic	T-12	2	WE+FVFG	Low	97	97	CDF
7	14	F	Femur	IIB	Fibroblastic	NSH-7	2	WE+FVFG	Negative	119	119	CDF
8	14	M	Fibula	IIB	Chondroblastic	NSH-7	2	WE	High	34	102	NED
9	11	F	Tibia	IIB	Osteoblastic	NSH-7	2	WE+FVFG	Negative	117	117	CDF
10	42	F	Tibia	IIB	Osteoblastic	NSH-7	2	WE+Prosthesis	High	72	72	CDF
11	14	M	Tibia	IIB	Osteoblastic	NSH-7	3	WE+FVFG	High	32	96	NED
12	18	M	2nd rib	IIB	Osteoblastic	NSH-7	0	WE	High	106	106	CDF
13	33	M	Pelvis	IIB	Chondroblastic	NECO93J	1	WE+FVFG	High	8	13	DOD
14	20	M	Femur	IIB	Fibroblastic	NECO93J	2	WE+FVFG	High	72	72	CDF
15	15	M	Femur	IIB	Osteoblastic	NECO93J	2	WE+FVFG	High	106	106	CDF
16	15	M	Femur	IIB	Osteoblastic	NECO93J	2	WE+FVFG	High	20	33	DOD
17	20	F	Femur	IIB	Osteoblastic	Not done†	(–)†	Not done†	Negative	0	7	DOD
18	16	M	Tibia	IIB	Chondroblastic	NECO93J	2	WE+FVFG	High	6	6	DOC‡
19	14	F	Femur	IIB	Osteoblastic	NECO93J	2	WE	Negative	5	5	DOC‡
20	15	M	Fibula	IIB	Osteoblastic	NECO93J	0	Amputation	High	13	74	DOD
21	13	M	Humerus	IIB	Chondroblastic	NECO93J	0	Amputation	High	7	9	DOD
22	7	F	Femur	IIB	Osteoblastic	NECO95J	1	WE+FVFG	High	85	85	CDF
23	10	F	Tibia	IIB	Osteoblastic	NECO95J	2	Amputation	Negative	72	72	CDF
24	13	M	Femur	IIB	Osteoblastic	NECO95J	0	WE+RP	Low	6	11	DOD
25	27	M	Tibia	IIB	Osteoblastic	NECO95J	0	WE+FVFG	High	8	18	DOD
26	18	F	Femur	IIIB	Fibroblastic	NECO95J	1	WE+Prosthesis	High	0	16	DOD
27	20	F	Humerus	IIB	Osteoblastic	NECO95J	2	WE+Prosthesis	Negative	67	67	CDF
28	69	F	Femur	IIB	Fibroblastic	NECO95J	0	WE+Prosthesis	Low	62	63	NED
29	15	F	Femur	IIB	Osteoblastic	NECO95J	3	WE+FVFG	High	32	32	CDF
30	46	M	Pelvis	IIB	Fibroblastic	NECO95J	0	WE+Fillet	Low	47	60	NED
31	40	F	Femur	IIB	Fibroblastic	NECO95J	2	Amputation	Low	12	20	DOD
32	19	M	Tibia	IIB	Osteoblastic	NECO95J	2	Amputation	High	41	43	DOD
33	15	F	Femur	IIB	Fibroblastic	NECO95J	3	WE+FVFG	High	52	52	CDF
34	48	M	Femur	IIB	Osteoblastic	NECO95J	2	Amputation	High	17	37	DOD
35	15	F	Femur	IIIB	Chondroblastic	NECO95J	1	WE+FVFG	High	0	17	NED
36	42	F	Sacrum	IIB	Osteoblastic	NECO95J	(–)§	Not done§	High	0	18	NED
37	7	M	Tibia	IIB	Osteoblastic	CCCH2	1	WE+RP	Low	13	86	DOD
38	12	F	Femur	IIB	Chondroblastic	CCCH2	0	Amputation	Low	5	84	DOD
39	17	M	Tibia	IIB	Chondroblastic	CCCH2	1	WE+RP	High	180	180	CDF
40	14	F	Femur	IIB	Fibroblastic	CCCH2	0	WE+Prosthesis	High	13	167	NED
41	19	M	Tibia	IIB	Fibroblastic	CCCH2	0	WE+RP	Low	20	36	DOD
42	14	F	Tibia	IIB	Osteoblastic	CCCH2	0	WE+Prosthesis	Low	19	44	DOD
43	12	M	Tibia	IIB	Osteoblastic	CCCH2	2	WE+Prosthesis	High	167	167	CDF
44	22	M	Femur	IIB	Fibroblastic	NECO93J	3	WE+RP	Low	164	164	CDF
45	21	M	Femur	IIB	Chondroblastic	NECO93J	1	WE+RP	High	34	80	DOD
46	20	M	Tibia	IIB	Osteoblastic	NECO93J	1	WE+RP	High	37	131	NED
47	17	M	Femur	IIB	Osteoblastic	NECO93J	3	WE+FVFG	High	127	127	CDF
48	8	F	Humerus	IIB	Osteoblastic	NECO93J	3	WE+FVFG	Low	126	126	CDF
49	20	F	Humerus	IIB	Fibroblastic	NECO93J	1	WE+FVFG	High	126	126	CDF
50	16	F	Femur	IIB	Osteoblastic	NECO93J	2	WE+RP	High	124	124	CDF
51	18	M	Tibia	IIB	Osteoblastic	NECO93J	0	WE+RP	Low	10	15	DOD
52	13	F	Femur	IIB	Osteoblastic	NECO95J	1	WE+Prosthesis	Low	100	100	CDF
53	11	M	Tibia	IIB	Chondroblastic	NECO93J	2	WE+RP	High	121	121	CDF
54	12	F	Tibia	IIB	Osteoblastic	NECO95J	1	WE+Prosthesis	High	114	114	CDF
55	24	M	Femur	IIB	Osteoblastic	NECO95J	1	WE+Prosthesis	Negative	79	79	CDF
56	14	F	Humerus	IIB	Chondroblastic	NECO95J	1	WE+FVFG	High	29	96	NED
57	26	M	Tibia	IIB	Osteoblastic	NECO95J	0	WE+Prosthesis	High	89	89	CDF
58	17	M	Radius	IIB	Osteoblastic	NECO95J	1	WE+FVFG	Low	84	84	CDF
59	18	F	Femur	IIB	Chondroblastic	NECO95J	1	WE+Prosthesis	High	17	69	DOD
60	15	M	Femur	IIB	Osteoblastic	NECO95J	2	WE+Prosthesis	Low	75	75	CDF
61	17	M	Femur	IIB	Osteoblastic	NECO95J	2	WE+Prosthesis	Low	74	74	CDF
62	13	M	Femur	IIB	Osteoblastic	NECO95J	2	WE+Prosthesis	Low	72	72	CDF
63	11	F	Femur	IIB	Osteoblastic	NECO95J	3	WE+Prosthesis	Low	66	66	CDF

Table 1. *Continued*

Patients	Age	Gender	Location	Surgical stage	Histological type	Chemotherapy	Histological response grade	Operation	PBF expression	EFS (months)	OS (months)	Prognosis
64	13	M	Femur	IIB	Osteoblastic	NECO95J	2	WE+Prosthesis	High	65	65	CDF
65	13	M	Femur	IIB	Osteoblastic	NECO95J	2	WE+Prosthesis	Negative	57	57	CDF
66	19	F	Femur	IIB	Osteoblastic	NECO95J	1	WE+Prosthesis	High	54	54	CDF
67	24	M	Tibia	IIB	Fibroblastic	NECO95J	0	WE+Prosthesis	Low	45	45	CDF
68	14	F	Femur	IIB	Osteoblastic	NECO95J	2	WE+Prosthesis	High	48	48	CDF
69	15	F	Femur	IIB	Osteoblastic	NECO95J	1	WE+Prosthesis	Low	7	18	DOD
70	19	M	Radius	IIB	Osteoblastic	NECO95J	1	WE+FVFG	Low	27	35	NED
71	16	F	Fibula	IIB	Osteoblastic	NECO95J	2	WE+Prosthesis	Low	33	33	CDF
72	10	M	Tibia	IIB	Osteoblastic	NECO95J	2	Amputation	High	12	32	AWD
73	11	M	Femur	IIB	Osteoblastic	NECO95J	1	WE+FVFG	Low	31	31	CDF
74	29	F	Fibula	IIB	Osteoblastic	NECO95J	1	WE	High	25	25	CDF
75	10	M	Femur	IIB	Chondroblastic	NECO95J	0	WE+Prosthesis	High	9	20	DOD
76	8	M	Femur	IIB	Osteoblastic	NECO95J	1	WE+RP	High	6	19	AWD
77	20	F	Tibia	IIB	Osteoblastic	NECO95J	2	Amputation	High	16	16	CDF
78	12	M	Femur	IIB	Osteoblastic	NECO95J	3	WE+Prosthesis	Low	15	15	CDF
79	65	M	Tibia	IIB	Osteoblastic	NECO95J[¶]	(–)[§]	WE+Prosthesis	High	2	13	NED
80	20	M	Femur	IIB	Osteoblastic	NECO95J	2	WE+Prosthesis	High	12	12	CDF
81	16	M	Ilium	IIB	Osteoblastic	NECO95J	1	WE	High	13	13	CDF
82	12	M	Femur	IIB	Osteoblastic	NECO95J	2	Amputation	High	8	13	DOD
83	20	M	Femur	IIB	Osteoblastic	NECO95J	2	WE+Prosthesis	High	12	12	CDF

[¶]Chemotherapy and operation were refused by the patient and her family. [§]Died of acute hepatitis B during postoperative chemotherapy. [§]Carbon ion radiotherapy was chosen instead of operation. [¶]Chemotherapy was instituted only postoperatively. AWD, alive with disease; CDF, continuously disease free; DOC, death of other cause; DOD, death of disease; EFS, event-free survival; F, female, FVFG, free vascularized fibula graft; M, male; NED, no evidence of disease; OS, overall survival; RP, rotational plasty; PBF, papillomavirus binding factor; WE, wide excision.

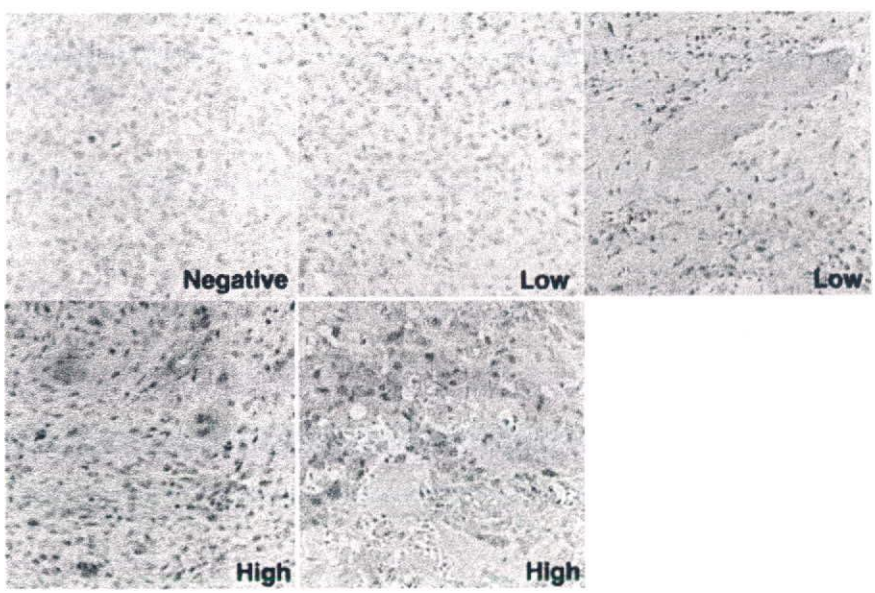

Fig. 1. Immunohistochemical grading of tumor specimens. Representative sections of osteosarcoma specimens stained with an anti-papillomavirus binding factor antibody are shown (original magnification ×200). Negative indicates that less than 5% of tumor cells were stained positively. Low indicates a positive tumor cell number from 5% to 50%. High indicates a positive tumor cell number of over 50%.

Survivorship analysis. Survivorship analysis was performed for 78 patients with osteosarcoma who had completed the protocols consisting of pre- and postoperative chemotherapy and underwent resection of the primary tumor with wide margin or amputation (Table 1). Five patients excluded were due to refusal (Patient 17) or incompletion of the chemotherapy (Patients 18, 19, and 79) and choice of non-surgical treatment (Patient 36). There were 43 males and 35 females with an average age of 17.9 years. Primary tumors were located in the femur (41 patients), tibia (19 patients), humerus (8 patients), fibula (4 patients), pelvis (3 patients), radius (2 patients) and rib (1 patient). According to Enneking's surgical staging system,[18] 76 patients were stage IIB and 2 patients were stage IIIB. There were 53 osteoblastic, 12 chondroblastic, 12 fibroblastic and 1 teleangiectatic osteosarcomas. Adjuvant chemotherapy protocols comprised of high-dose methotrexate-based multidrug regimen, including T-12,[19] NSH-7,[20] CCCH2,[21] NECO93J,[22] and NECO95J.[23,24] The responses of the tumors to preoperative chemotherapy were histologically graded according to the classification of the Japanese Orthopaedic Association:[25] Grade 0 (tumor necrosis <50%), 1 (≤50% tumor necrosis <90%), 2 (tumor necrosis ≥90%), 3 (No viable tumor cells in the histological sections). These 78 patients were followed up for an average of 65.0 months (range from 9 to 180 months).

The prognostic significance of the following variables overall and in the event-free survival of patients with osteosarcoma was

doi: 10.1111/j.1349-7006.2008.00695.x

Table 2. Sequences and binding affinities of PBF-derived peptides with HLA-A*2402 binding motif

Peptide	Position	Sequence	Binding score[†]	HLA-peptide binding affinity[‡] (% MFI increase ± SD)
A24.1	84–93	WYGGQECTGL	200	−3.0 ± 3.2
A24.2	145–153	AYRPVSRNI	84	119.2 ± 7.3
A24.3	409–418	AYQALPSFQI	75	25.3 ± 6.0
A24.4	254–263	GFETDPDPFL	30	2.6 ± 10.3
A24.5	320–328	DFYYTEVQL	20	2.3 ± 9.6
A24.6	118–127	RVEEVWLAEL	15.8	22.5 ± 9.6
A24.7	254–262	GFETDPDPF	15	−1.2 ± 5.9
A24.8	12–20	RSLLGARVL	12	14.2 ± 5.8
A24.9	415–424	SFQIPVSPHI	10.5	11.7 ± 7.9
A24.10	104–113	VTVWILEQKL	9.5	7.1 ± 1.2
HIV		RYLRDQQLLGI		41.2 ± 9.3

[†]Binding score was determined by BIMAS HLA Peptide Binding Predictions. [‡]The affinity of each peptide was evaluated by a HLA class I stabilization assay. BIMAS, bioinformatics and molecular analysis section; HLA, human leukocyte antigen; MFI, mean fluorescence intensity; PBF, papillomavirus binding factor; SD, standard deviation.

determined by univariate analysis using the generalized Wilcoxon test: age (≥ 15), gender (male or female), stage (IIB or IIIB), histological type (osteoblastic, chondroblastic or fibroblastic), response to chemotherapy (Grades 0 and 1 or Grades 2 and 3), and PBF expression status (negative, low or high). The relationship between each variable and PBF expression status was determined by the chi-squared test. A probability of less than 0.05 was considered statistically significant.

Cell lines. An osteosarcoma cell line, OS2000, and an Epstein–Barr virus-transformed B cell line, LCL-OS2000, were established previously from a 17-year-old patient.[11] Osteosarcoma cell lines HOS and U2OS, and the erythroleukemia cell line K562 were purchased from American Type Culture Collection (Manassas, VA, USA). OS2000, HOS, U2OS and K562 were PBF$^+$ and LCL-OS2000 was PBF$^-$.[12] The HLA genotypes of osteosarcoma cell lines were as follows: OS2000, A*2402, B*5502, B*4002, Cw*0102; HOS, A*0211, B*5201, Cw*1202; U2OS, A*0201, A*3201, B*4402, Cw*0501, Cw*0704.

Design and synthesis of PBF-derived peptides. Based on the entire amino acid sequence of PBF, peptides with the ability to bind to HLA-A24 class I molecules were searched through the Internet site, Bioinformatics and Molecular Analysis Section (BIMAS) HLA Peptide Binding Predictions (http://bimas.cit.nih.gov/).[26] Based on the binding scores, 10 peptides were selected and synthesized (Table 2).

HLA class I stabilization assay. The affinity of peptides for HLA-A24 molecules was evaluated by cell surface HLA class-I stabilization assay as described previously.[27,28] An HLA-A*2401-binding HIV peptide (RYLRDQQLLGI) was used for positive control. Assays were performed in triplicate. The affinity of each peptide for HLA-A*2402 molecules was evaluated by the percent mean fluorescence intensity (%MFI) increase of the HLA-A*2402 molecules in the calculation: %MFI increase: [(MFI with the given peptide − MFI without peptide)/(MFI without peptide)] × 100.

Limiting dilution/mixed lymphocyte peptide culture. Prior to frequency analysis and cytotoxicity assays, peripheral blood mononuclear cell (PBMC) of patients were subjected to mixed lymphocyte peptide culture under limiting dilution conditions (LD/MLPC) according to the method described by Karanikas *et al.*[29] with some modifications. For frequency analysis, peripheral blood samples (20 mL) were collected from nine patients with PBF$^+$ osteosarcoma (Patient 26, 36, 76, 78–83) (Table 1). PBMC were suspended in AIM-V (Invitrogen Crop., Carlsbad, CA, USA) supplemented with 1% human serum (HS) and incubated for 60 min at room temperature with PBF A24.2 peptide (25 μg/mL). Peptide-pulsed PBMC were seeded at 2×10^5 cells/200 μL/well into round-bottom 96-microwell plates in AIM-V with 10%HS, IL-2 (20 U/mL; a kind gift from Takeda Chemical Industries Ltd, Osaka, Japan) and IL-7 (10 ng/mL; R & D Systems, Minneapolis, MN, USA), and incubated. On day 7, half of the medium was replaced by fresh AIM-V containing IL-2, IL-7 and the same peptides. The cell cultures were maintained by adding fresh AIM-V containing IL-2. On days 14–21, they were subjected to tetramer-based frequency analysis.

For cytotoxicity assays, PBMC of Patient 36 were separated into CD8$^+$ cells and CD8$^-$ cells using magnetic anti-CD8 microbeads (Miltenyi Biotec, Gladbach, Germany). CD8$^-$ cells were pulsed with the PBF A24.2 peptide for 60 min. Half of the CD8$^-$ cells were cryopreserved at −80°C for the second stimulation. CD8$^+$ cells (2.5×10^5/well) and irradiated PBF A24.2 peptide-pulsed CD8$^-$ cells (5×10^5/well) were cocultured in 37 wells of a 48-well cell culture plate in 500 μL of AIM-V with 10%HS, IL-2 and IL-7. On day 7, the second stimulation was performed by adding irradiated peptide-pulsed CD8$^-$ cells to each culture well in 500 μL of freshly replaced AIM-V with 10%HS, IL-2 and IL-7. On day 14–28, they were subjected to tetramer-based cytotoxicity assays.

Tetramer-based frequency analysis. An fluorescein isothiocyanate-conjugated HLA-A24/HIV tetramer (here termed the control tetramer) and a phycoerythrin (PE)-conjugated HLA-A24/PBF A24.2 tetramer (A24/PBF A24.2 tetramer) were constructed by Medical & Biological Laboratories Co. Ltd. (Tokyo, Japan). PBMC from patients were stimulated with the PBF A24.2 peptide by LD/MLPC as described above. From each microwell containing 200 μL of the microculture pool, 100 μL was transferred to a V-bottom microwell and washed. On the spin-down pellets, the control tetramer and A24/PBF A24.2 tetramer (10 nM in 25 μL of phosphate-buffered saline (PBS)) were added in combination and incubated for 15 min at room temperature. Then a PE-Cy5-conjugated anti-CD8 antibody (eBioscience, San Diego, CA, USA) was added (dilution of 1:30 in 25 μL of PBS containing the control tetramer and A24/PBF A24.2 tetramer) and incubated for another 15 min. The cells were washed in PBS twice, fixed with 0.5% formaldehyde, and analyzed by flow cytometry using FACScan and CellQuest software (Becton Dickinson, San Jose, CA, USA). CD8$^+$ living cells were gated and the cells labeled with the A24/PBF A24.2 tetramer and non-labeled cells with the control tetramer were referred to as tetramer-positive cells. The frequency of anti-PBF A24.2 CTLs was evaluated using the following calculation: (number of tetramer-positive wells)/([numbers of total tested wells] × [number of CD8$^+$ cells per well]).

Tetramer-based cytotoxicity assay. CTL-mediated cytolytic activity was measured by a 6 h-^{51}Cr release assay.[30] Osteosarcoma cell lines (OS2000, HOS and U2OS), EB-transformed B cell line LCL-OS2000 and K562 were used as the target cells. OS2000 was treated with and without 100 U/mL interferon-gamma (R & D Systems, Minneapolis, MN, USA) for 48 h. LCL-OS2000 was also treated with and without peptides (25 μg/mL) for 2 h at room temperature before assay. Target cells were labeled with 100 μCi of ^{51}Cr for 1 h at 37°C. The labeled target cells were suspended in Dulbecco's modified eagle's medium containing 10% fetal calf serum and seeded to microwells (2×10^3 cells/well). Patient 36-derived CD8$^+$ CTL lines stimulated with the PBF A24.2 peptide by LD/MLPC were used as the effector cells. Tetramer-positive CTL lines were transferred to V-bottom microwells, suspended in AIM-V and mixed with the labeled target cells. In cold-target inhibition assays, a 100-fold excess of unlabeled PBF A24.2-pulsed target cells was added as cold target cells. After a 6 h incubation period at 37°C, the release of the ^{51}Cr level in the supernatant of the culture was measured by quantification in an automated gamma

Table 3. Univariate analysis of variables in event-free survial and overall survival

Variables		*n*	Event-free survival (months in average)	*P*-value	Overall survival (months in average)	*P*-value
Age	≤15	41	49.6	0.215	66.8	0.949
	>15	37	54.7		63	
Gender	Male	46	48.5	0.244	64.4	0.101
	Female	32	57.1		70.8	
Stage	IIB	76	53.4	0.006	66.3	0.062
	IIIB	2	0		16.5	
Histological type	Osteoblastic	53	52.1	0.052*	60.7	0.461*
	Chondroblastic	12	38.2	<0.001*	67.7	0.105*
	Fibroblastic	12	61.0	0.899*	78.3	0.665*
	Teleangiectatic	1	103.4			
Response to chemotherapy	Grades 0,1	41	40.5	<0.001	60.2	0.007
	Grades 2,3	37	64.7		70.3	
PBF status	Positive	72	49.2	0.025	63.3	0.091
	Negative	6	85.2		85.2	

*P-value was determined in comparison with the survival of patients with other subtypes.

Table 4. Clinical picture and frequency of anti-PBF A24.2 peptide CTLs in PBMC of patients with PBF-positive osteosacoma

Participants	Status of tumor bearing	Chemotherapy	Total number of tested wells	Number of tetramer-positive wells	Number of PMBC	%CD8	Number of $CD8^+$ cells per pool	Frequency†
Patient								
26	(P)‡, M	underway	62	14	200 000	17	34 000	7×10^{-6}
36	P	not done	194	6	210 000	23	48 000	6×10^{-7}
76	(P)	underway	19	2	200 000	9	18 000	6×10^{-6}
78	(P)	underway	62	1	200 000	15	30 000	5×10^{-7}
79	(P), M	underway	28	0	200 000	15	30 000	$<1 \times 10^{-6}$
80	(P)	underway	160	15	290 000	20	58 000	2×10^{-6}
81	(P)	underway	149	5	200 000	3	6000	6×10^{-6}
82	(P)	underway	132	3	200 000	4	8000	3×10^{-6}
83	P	underway	40	5	200 000	25	50 000	3×10^{-6}

†Frequency of anti-PBF A24.2 CTLs among $CD8^+$ cells. ‡Parentheses indicate that the tumor had been present previously but was free at the time blood sample was taken. CTLs, cytotoxic T lymphocytes; M, metastatic tumor; P, primary tumor; PBF, papillomavirus binding factor; PMBC, peripheral blood mononuclear cell.

counter. The percentage of specific cytotoxicity was calculated as the percentage of specific ^{51}Cr release: 100 × (experimental release – spontaneous release)/(maximum release – spontaneous release). The cytotoxicity rate to OS2000 was calculated as (%cytotoxicity to each target cells)/(%cytotoxicity to OS2000).

Results

Expression of PBF protein in osteosarcoma. To determine the prevalence of the osteosarcoma-derived antigen PBF protein in osteosarcomas, we stained formalin-fixed paraffin-embedded sections of 83 specimens with a polyclonal antibody against PBF (Table 1 and Fig. 1). Of these, 76 specimens (92%) were positively stained with the anti-PBF antibody, including 49 specimens (59%) with high-grade staining.

Prognostic impact of PBF expression in patients with osteosarcoma. We then analyzed the prognostic significance of several variables including expression of PBF, in 78 patients with osteosarcoma who completed chemotherapy protocols and had wide tumor excision (Table 1). As depicted in Table 3, patients with chondroblastic type osteosarcoma showed significantly poorer event-free survival rate than those with other histological types. Forty-one patients with osteosarcoma showing a poor response to preoperative chemotherapy (Grades 0 and 1) showed significantly more unfavorable event-free and overall survival rates than 37 good responders (Grades 2 and 3). With respect to PBF-expression status, 72 patients with positive expression of PBF in the primary tumor were significantly more unfavorable in event-free survival than six patients with PBF-negative osteosarcoma ($P = 0.025$). This finding was consistent in subgroup analysis with 46 patients with high-grade PBF expression and 26 patients with low-grade PBF expression ($P = 0.026$ and 0.032, respectively). In contrast, age and gender failed to have significant prognostic impacts on event-free and overall survival rates of the patients.

Subsequently, we analyzed the relationship between the PBF-expression status in osteosarcoma and other variables. PBF-expression status was not significantly related to any variables including age ($P = 0.472$), gender ($P = 0.184$), stage ($P = 0.694$), histological type ($P = 0.743$) and the response to chemotherapy ($P = 0.069$).

Affinity of PBF-derived synthetic peptides to HLA-A*2402 molecules. To determine the immunogenicity of PBF in patients with HLA-A24, we synthesized 10 peptides from the PBF sequence in accordance with the BIMAS score for HLA-A24 affinity (Table 2). Subsequently, we evaluated the affinities of these peptides to HLA-A24 molecules by the HLA class-I stabilization assay. As shown in Table 2, peptide PBF A24.2 showed the highest MFI increases in the context of HLA-A24.

Frequency of anti-PBF A24.2 CTLs in $HLA\text{-}A24^+$ patients with osteosarcoma. We then examined the frequency of peripheral $CD8^+$ T-lymphocytes that recognized the PBF A24.2 peptide in 9 $HLA\text{-}A24^+$ patients with PBF^+ osteosarcoma by LD/MLPC/tetramer analysis. As depicted in Table 4 and representatively shown in Fig. 2(a),

doi: 10.1111/j.1349-7006.2008.00695.x

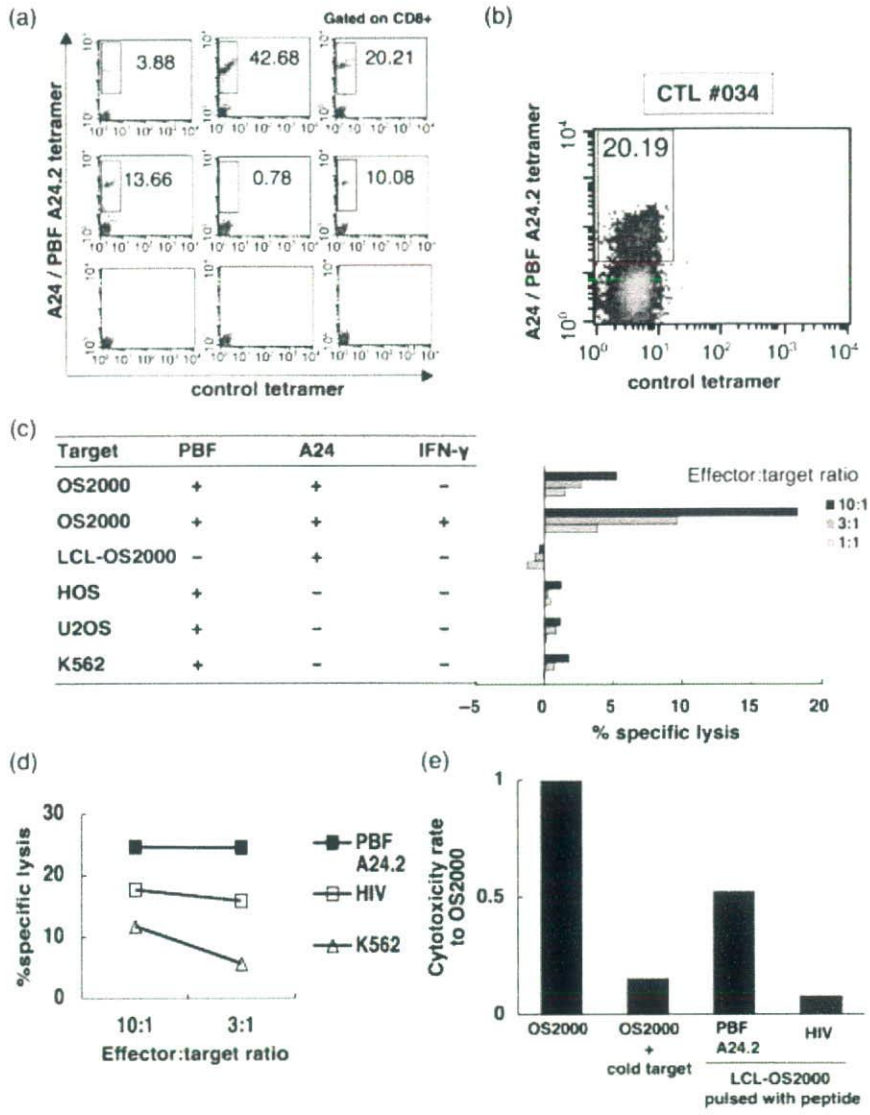

Fig. 2. Tetramer-based detection of anti-PBF A24.2 peptide CTLs in peripheral blood of patients with osteosarcoma. (a) peripheral blood mononuclear cell of Patient 26 were seeded into 62 microwells and stimulated with the papillomavirus binding factor (PBF) A24.2 peptide by mixed lymphocyte peptide culture under limiting dilution conditions (LD/MLPC). The resultant cytotoxic T lymphocytes (CTL) pools were stained with the phycoerythrin (PE)-conjugated A24/PBF A24.2 tetramer, fluorescein isothiocyanate-conjugated control tetramer, and a PE-Cy5-conjugated anti-CD8 mAb. Cells reacting with the anti-CD8 mAb were gated. The reactivity of gated cells with the A24/PBF A24.2 tetramer and the control tetramer are shown. The upper and middle columns display six representative pools with positive reactivity to the A24/PBF A24.2 tetramer. The cells labeled with the A24/PBF A24.2 tetramer and non-labeled cells with the control tetramer were considered to be tetramer-positive cells and are boxed to show their proportion among $CD8^+$ cells. The bottom row shows three negative pools. (b) $CD8^+$ cells (2.5×10^5 cells/well) of Patient 36 were seeded into 37 wells of a 48-well culture plate and stimulated with irradiated peptide-pulsed $CD8^-$ cells (5×10^5 cells/well) by LD/MLPC. Tetramer analysis was performed on day 14. The results of one of the four tetramer-positive CTL line (CTL #034) in the 37 pools are shown. Cells reacting with the anti-CD8 mAb were gated. The tetramer-positive cells are boxed to show their proportion among $CD8^+$ cells. (c) The cytotoxicity of CTL #034 against allogeneic osteosarcoma cell lines (OS2000, HOS, U2OS), LCL-OS2000 and K562 was assessed by a 6 h standard ^{51}Cr release assay at the indicated effector:target ratios. OS2000 was assayed in the presence and absence of 48 h-interferon-gamma pretreatment. (d) The cytotoxicity of CTL #034 against peptide-pulsed LCL-OS2000 and K562 was assessed by a 6 h standard ^{51}Cr release assay at the indicated effector:target ratios. LCL-OS2000 was pulsed with 25 μg/mL of PBF A24.2 peptide or HIV control peptide for 2 h at room temperature before labeling with ^{51}Cr. (e) Cold target inhibition assay. The cytotoxicity of CTL #034 against interferon-gamma-treated, ^{51}Cr-labeled OS2000 was assessed in the presence and absence of a 100-fold excess of PBF A24.2 peptide-pulsed, cold LCL-OS2000 at a 10:1 effector-target ratio. ^{51}Cr-labeled LCL-OS2000 cells pulsed with the PBF A24.2 peptide or HIV peptide were also used as control target cells.

anti-PBF A24.2 CTLs were detected as tetramer-positive cells in eight of the nine patients with osteosarcoma. The frequencies of anti-PBF A24.2 CTLs were between 5×10^{-7} and 7×10^{-6} (4×10^{-6} in average) in eight tetramer-positive patients.

Tetramer-based cytotoxicity of anti-PBF A24.2 CTLs against osteosarcoma cell lines. Finally we assessed the cytotoxic activity of tetramer-positive cells against allogeneic osteosarcoma cell lines. We induced tetramer-positive anti-PBF A24.2 CTLs from 1×10^7 $CD8^+$ cells of Patient 36 by LD/MLPC using 48-well culture plates. Irradiated peptide-pulsed $CD8^-$ cells were used as stimulator cells. As a result, 4 of 37 tetramer-positive CTLs were detected by tetramer analysis on day 14. Four tetramer-positive CTLs contained 3.47%, 0.03%, 15.26% and 20.19%. One of four CTL lines (CTL #034) was shown in Fig. 2(b).

The cytotoxicity against OS2000 (PBF^+, $A24^+$), LCL-OS2000 (PBF^-, $A24^+$), HOS (PBF^+, $A24^-$), U2OS (PBF^+, $A24^-$) and K562 (PBF^+, HLA class I loss) was comparatively assessed by ^{51}Cr release assay. As depicted in Fig. 2(c), CTL #034 showed specific cytotoxicity against OS2000 and the cytotoxicity was enhanced by interferon-gamma pretreatment. In contrast, none of these CTL lines exhibited cytotoxic activity against LCL-OS2000, HOS, U2OS, or K562 cells. The other three tetramer-positive CTL lines also showed specific cytotoxicity against OS2000 (data not shown).

We subsequently determined the specificity of cytotoxicity with the PBF A24.2 peptide by using peptide-pulsed LCL-OS2000. As shown in Fig. 2(d), CTL #034 lyzed PBF A24.2 peptide-pulsed LCL-OS2000 more than control peptide (HIV)-pulsed LCL-OS2000 or K562 cells. Peptide-specific cytotoxicity of CTL #034 was also assessed by cold-target inhibition assay (Fig. 2e). Cytotoxicity against OS2000 pretreated with interferon-gamma was inhibited by adding a 100-fold excess of cold LCL-OS2000 pulsed with PBF A24.2.

Discussion

In the present study, we examined the distribution profile, prognostic impact, and immunogenicity of the novel tumor-associated antigen PBF in osteosarcoma. We found: (i) that 92% of 83 osteosarcoma specimens expressed PBF protein; (ii) that PBF-positive osteosarcomas conferred a significantly poorer prognosis than those with negative expression of PBF in event-free

survival of 78 patients who completed the standard treatment; (iii) that $CD8^+$ T cells reacting with a PBF-derived HLA-A24-binding peptide (PBF A24.2 peptide) were detected in eight out of nine HLA-A24-positive patients with osteosarcoma at the frequency from 5×10^{-7} to 7×10^{-6}; and (iv) that PBF A24.2 peptide induced CTL lines from an HLA-A24-positive patient, which specifically killed an osteosarcoma cell line that expresses both PBF and HLA-A24. These findings suggest the oncogenic and antigenic role of PBF in patients with osteosarcoma, especially those with HLA-A24. The proof of immunogenicity of PBF has been limited to an HLA-B55-positive patient with osteosarcoma.[12] Wide distribution of PBF in osteosarcoma and the immunogenicity of PBF seen in patients with HLA-A24 extended the possibility of PBF-targeted immunotherapy against osteosarcoma. Patients with negative expression of PBF in osteosarcoma can be treated successfully by the current chemotherapy-based treatment protocols.

To date, peptide-based immunotherapy in patients with bone and soft tissue sarcomas has been reported only with the use of fusion gene-derived peptides.[31,32] This approach has been available for tumors in which specific chromosomal translocations have been identified, including synovial sarcoma and Ewing sarcoma. However, for other sarcomas including osteosarcoma, where chromosomal translocation and a resultant fusion gene have not been identified, novel tumor-associated antigens need to be defined. With this aim, we developed autologous pairs of tumor cells and CTLs from patients with sarcomas. Consequently, PBF was identified from an autologous osteosarcoma-CTL pair. PBF protein was defined in 89% of the various bone and soft tissue sarcomas (Tsukahara *et al.* 2004, unpub. data). Therefore, the PBF A24.2 peptide might be applicable to immunotherapy against bone and soft tissue sarcomas without known chromosomal translocations, other than osteosarcoma.

Our univariate analysis revealed prognostic significance of PBF in event-free survival. Such prognostic values need to be verified by multivariate analysis. In this regard, all of the six patients with PBF-negative osteosarcoma analyzed are continuously disease-free. Unfortunately, the disproportional profile of these patients caused failure in multivariate analysis. In contrast, poor response to chemotherapy and chondroblastic subtype remained significant in the multivariate analysis (Tsukahara *et al.* 2007, unpub. data), indicating the validity of the patient population in the present analysis. The unfavorable prognostic value of PBF was also seen in our analysis with 20 patients with Ewing sarcoma.[33]

The frequency of anti-PBF CTL precursor was determined between 5×10^{-7} and 7×10^{-6}. In melanoma patients, the anti-MAGE3.A1 CTL precursor frequency was estimated to be $<10^{-7}$ in normal donors and prevaccinated patients, and 10^{-6} in postvaccinated patients.[34] Although the anti-PBF A24.2 peptide CTL precursor frequency defined in the present study was relatively higher than the anti-MAGE3.A1 CTL frequency, it was still under the detection level of the standard tetramer analysis and thus required the LD/MLPC/tetramer procedure for detection. The LD/MLPC/tetramer procedure was advantageous with its high sensitivity for the frequency analysis of peptide-specific CTLs in preclinical studies and clinical trials.[35,36] Also, this procedure served as prescreening of CTLs for subsequent cytotoxicity analysis. However, the multistep procedure of LD/MLPC/tetramer analysis requires labor-intensive laboratory work and long-term cell culture.[37,38] This gives rise to a concern about possible changes in the effector function and differentiation status of CTLs during the analysis.[39,40]

Cytotoxicity of CTL induced with PBF A24.2 peptide was proved only in an osteosarcoma cell line that is positive for PBF and HLA-A24. It would be ideal to conduct cytotoxicity assays with more number of cell lines. However, limited cell numbers of CTL lines expanded after LD/MLPC/tetramer analysis made it difficult to carry out. Instead, we examined the specificity of the cytotoxicity by peptide-pulsation as well as cold inhibition assays.

In conclusion, the present study demonstrated the feasibility and population of candidates for PBF-targeted immunotherapy for osteosarcoma. The combination of LD/MLPC with tetramer labeling as well as ^{51}Cr release cytotoxicity assay enables us to concurrently determine the frequency and function of CTL precursors, and thus serves as a useful tool for identification of novel antigenic peptides and immunomonitoring in clinical immunotherapy trials.

Acknowledgments

We thank Drs Pierre G. Coulie and Tomoko So for their kind advice about the LD/MLPC/tetramer procedure, Dr Hideo Takasu for the kind donation of synthetic peptides and Drs Naoki Hatakeyama and Takeshi Terui for their clinical support with chemotherapy and donation of blood samples.

References

1 Ferrari S, Smeland S, Mercuri M *et al.* Neoadjuvant chemotherapy with high-dose ifosfamide, high-dose methotrexate, cisplatin, and doxorubicin for patients with localized osteosarcoma of the extremity: a joint study by the Italian and Scandinavian Sarcoma Groups. *J Clin Oncol* 2005; **23**: 8845–52.
2 Lewis VO. What's new in musculoskeletal oncology. *J Bone Joint Surg Am* 2007; **89**: 1399–407.
3 Campbell CJ, Cohen J, Enneking WF. Editorial: New therapies for osteogenic sarcoma. *J Bone Joint Surg Am* 1975; **57**: 143–4.
4 Kawaguchi S, Wada T, Tsukahara T *et al.* A quest for therapeutic antigens in bone and soft tissue sarcoma. *J Transl Med* 2005; **3**: 31.
5 Meyers PA, Schwartz CL, Krailo M *et al.* Osteosarcoma: a randomized, prospective trial of the addition of ifosfamide and/or muramyl tripeptide to cisplatin, doxorubicin, and high-dose methotrexate. *J Clin Oncol* 2005; **23**: 2004–11.
6 Maki RG. Future directions for immunotherapeutic intervention against sarcomas. *Curr Opin Oncol* 2006; **18**: 363–8.
7 Mocellin S, Mandruzzato S, Bronte V, Lise M, Nitti D, Part I. Vaccines for solid tumours. *Lancet Oncol* 2004; **5**: 681–9.
8 van Baren N, Bonnet MC, Dreno B *et al.* Tumoral and immunologic response after vaccination of melanoma patients with an ALVAC virus encoding MAGE antigens recognized by T cells. *J Clin Oncol* 2005; **35**: 9008–21.
9 Thurner B, Haendle I, Roder C *et al.* Vaccination with MAGE-3A1 peptide-pulsed mature, monocyte-derived dendritic cells expands specific cytotoxic T cells and induces regression of some metastases in advanced stage IV melanoma. *J Exp Med* 1999; **190**: 1669–78.
10 Morgan RA, Dudley ME, Wunderlich JR *et al.* Cancer regression in patients after transfer of genetically engineered lymphocytes. *Science* 2006; **314**: 126–9.
11 Nabeta Y, Kawaguchi S, Sahara H *et al.* Recognition by cellular and humoral autologous immunity in a human osteosarcoma cell line. *J Orthop Sci* 2003; **8**: 554–9.
12 Tsukahara T, Nabeta Y, Kawaguchi S *et al.* Identification of human autologous cytotoxic T-lymphocyte-defined osteosarcoma gene that encodes a transcriptional regulator, papillomavirus binding factor. *Cancer Res* 2004; **64**: 5442–8.
13 Boeckle S, Pfister H, Steger G. A new cellular factor recognizes E2 binding sites of papillomaviruses which mediate transcriptional repression by E2. *Virology* 2002; **293**: 103–17.
14 Sichtig N, Silling S, Steger G. Papillomavirus binding factor (PBF)-mediated inhibition of cell growth is regulated by 14–3–3 beta. *Arch Biochem Biophys* 2007; **464**: 90–9.
15 Tsukahara T, Kawaguchi S, Ida K *et al.* HLA-restricted specific tumor cytolysis by autologous T-lymphocytes infiltrating metastatic bone malignant fibrous histiocytoma of lymph node. *J Orthop Res* 2006; **24**: 94–101.
16 Al-Batran SE, Rafiyan MR, Atmaca A *et al.* Intratumoral T-cell infiltrates and MHC class I expression in patients with stage IV melanoma. *Cancer Res* 2005; **65**: 3937–41.
17 Tsukahara T, Kawaguchi S, Torigoe T *et al.* Prognostic significance of HLA class I expression in osteosarcoma defined by anti-pan HLA class I monoclonal antibody, EMR8-5. *Cancer Sci* 2006; **97**: 1374–80.

doi: 10.1111/j.1349-7006.2008.00695.x